ANL-7532

Argonne National Laboratory

ELEMENTARY NEUTRONICS CONSIDERATIONS IN LMFBR DESIGN

by

G. H. Golden

The facilities of Argonne National Laboratory are owned by the United States Government. Under the terms of a contract (W-31-109-Eng-38) between the U. S. Atomic Energy Commission, Argonne Universities Association and The University of Chicago, the University employs the staff and operates the Laboratory in accordance with policies and programs formulated, approved and reviewed by the Association.

MEMBERS OF ARGONNE UNIVERSITIES ASSOCIATION

The University of Arizona	Kansas State University	The Ohio State University
Carnegie-Mellon University	The University of Kansas	Ohio University
Case Western Reserve University	Loyola University	The Pennsylvania State University
The University of Chicago	Marquette University	Purdue University
University of Cincinnati	Michigan State University	Saint Louis University
Illinois Institute of Technology	The University of Michigan	Southern Illinois University
University of Illinois	University of Minnesota	University of Texas
Indiana University	University of Missouri	Washington University
Iowa State University	Northwestern University	Wayne State University
The University of Iowa	University of Notre Dame	The University of Wisconsin

Printed in the United States of America
Available from
Clearinghouse for Federal Scientific and Technical Information
National Bureau of Standards, U. S. Department of Commerce
Springfield, Virginia 22151
Price: Printed Copy $3.00; Microfiche $0.65

ANL-7532
Reactor Technology

ARGONNE NATIONAL LABORATORY
9700 South Cass Avenue
Argonne, Illinois 60439

ELEMENTARY NEUTRONICS CONSIDERATIONS IN LMFBR DESIGN

by

G. H. Golden

Reactor Engineering Division

March 1969

TABLE OF CONTENTS

LIST OF FIGURES

LIST OF TABLES

NOMENCLATURE

Symbol	Description
A	Doppler coefficient, $T(dk/dT)_{Dop}$
C	rate of parasitic absorption of neutrons in reactor
E	energy corresponding to velocity of neutron relative to nucleus, ev or Mev
F	fraction of fissions that occur in fertile isotopes
J	total number of groups in a multigroup analysis
k_{eff}	reactor multiplication constant
L	net rate of neutron leakage from blanket
M	downscatter band in multigroup diffusion equations
M_c	core critical mass, kg of Pu-239 + Pu-241
N^m	atom density of mth nuclide, atoms/cm^3
P	total reactor power or core power, MW
$\overline{P}$	average core power density, kW/liter
$P_k(\vec{r})$	fission power density at point $\vec{r}$ in region k
P_s	core specific power, kW/kg
Q_k	total power in region k of reactor
R_e	extrapolated dimension, cm
T	average fuel temperature, °K
V_k	volume of kth region of reactor, liters
BR	reactor breeding ratio
BG	BR - 1, reactor breeding gain
CR	core conversion ratio
DT	doubling time, years
MWe	megawatts of electrical power
MWd	megawatt days of thermal energy
α	σ_c/σ_f, capture-to-fission ratio
β	delayed neutron fraction

NOMENCLATURE (Contd.)

Symbol	Description
ε	fraction of time reactor is at full power
ν	average number of neutrons, including delayed neutrons, emitted per fission
σ_x^m	microscopic cross section of isotope m for process x, cm^2
Σ	$N\sigma$, macroscopic cross section, cm^{-1}
$\phi(E,\vec{r})$	neutron flux per unit energy interval at space point $\vec{r}$
$\phi(t)$	neutron flux at time t, neutrons/cm^2 sec
$\chi(E)$	fission neutron distribution in energy

Subscripts:

k	kth region of reactor
a	absorption
c	radiative capture
f	fission
s	scattering
t	total
el	elastic
in	inelastic
tr	transport

Superscripts:

fp	fission product pairs

ABSTRACT

Elementary neutronics considerations in the design of liquid-metal-cooled fast breeder reactors (LMFBRs) are described to provide a basic understanding to the scientist or engineer who does not have a background in fast-reactor neutronics. The discussion is not intended to be either a rigorous treatment of the specialized subject of fast reactor physics, or an LMFBR design manual, so rigor is sacrificed frequently for clarity at the desired level. Thus many of the points made are "design-acceptable" approximations that are not absolutely accurate.

The subject material is a progression from basic physics concepts to the design of real LMFBRs: (1) flux spectra and cross-section variation with energy in fast reactors; (2) aspects of multigroup calculations in diffusion theory; (3) the significance of breeding and conversion ratios, specific power, and doubling time; (4) radial core zoning; (5) refueling (i.e., time-dependent behavior); (6) a discussion of reactivity effects as related to safety, with specific reference to sodium void, Doppler, and expansion effects; and (7) current design approaches.

Although the presentation is made within the framework of LMFBR design, it is applicable to the design of any fast breeder, regardless of coolant. Hence, pertinent comments have been made regarding gas-cooled fast breeder reactors.

ELEMENTARY NEUTRONICS CONSIDERATIONS IN LMFBR DESIGN

by

G. H. Golden

I. Introduction

In any reactor, steady-state operation represents a balance between neutron production by fission and loss by absorption and leakage. The fission neutrons are born at an energy of about 2 MeV. In a thermal reactor they are slowed down, primarily by elastic scattering in a moderator in which they approach thermal equilibrium. During the slowing-down process, some of the neutrons are lost by leakage, others by parasitic capture, and others by fission reactions. The surviving "thermalized" neutrons then cause fission of the primary fissile material, undergo parasitic capture, or are lost by leakage.

The thermal neutron flux per unit energy interval in a thermal reactor, $\phi(E)$, has a Maxwellian-like distribution in energy, with the location of the peak determined by the average temperature of the moderator. Figure 1 shows such a distribution.[1] Here for pure water moderator at 80°C the peak occurs at about 0.03 eV. Also shown in this figure is the "hardening" effect of absorber material on the spectrum, as well as the "1/E" behavior of the latter at higher energies.

In a fast reactor there is little moderating material, and hence little degradation of the flux spectrum. Here the flux peaks in the hundred keV region, as is shown for oxide, carbide and metal fuel LMFBRs in Fig. 2. Because the distributions in this figure were obtained directly from a multigroup analysis, the ordinate is not $\phi(E)$, but the group flux, a parameter that is approximately $E \cdot \phi(E)$.

The bigger a fast reactor is made, the more degraded or softer its spectrum becomes, because of increased inelastic and elastic scattering, relative to absorption and leakage. Figure 3 shows this effect for metal-fuel LMFBRs having core volumes of 1000, 3000, and 7000 liters. In large LMFBRs (4000-8000 liters), a small but important fraction of the flux is in the 1-keV region, as shown in Fig. 2. This region is significant because it contains resonances important to the Doppler effect (Section VI-C). Also, it is the region in which there is current uncertainty with regard to a

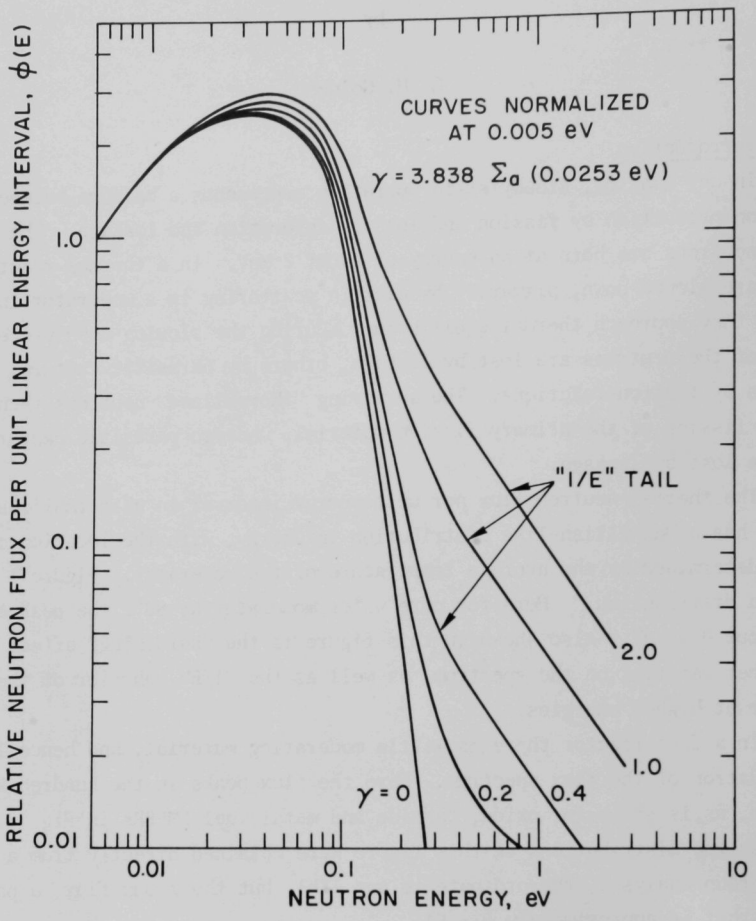

Fig. 1 Neutron distributions in H_2O at 80°C for different amounts of absorption.
Reproduced from: Brown, H. D., "Neutron Energy Spectra in Water" Dp-64, Feb. 1956; see Ref. 1, p. 90

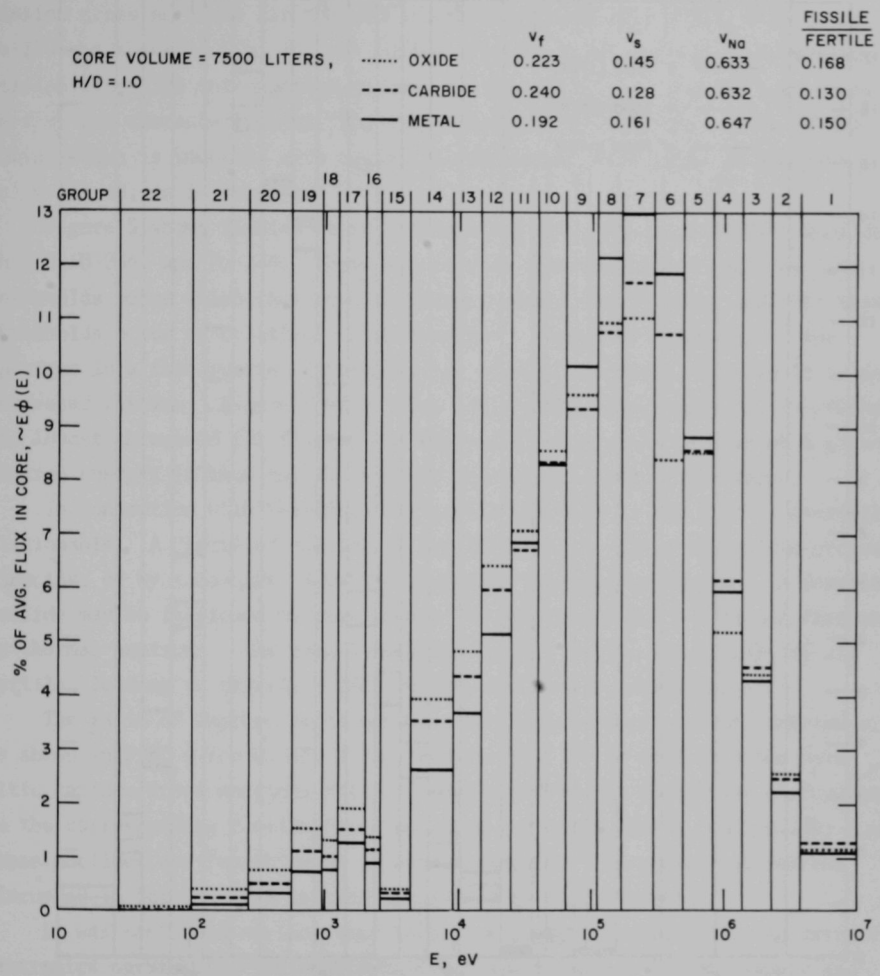

Fig. 2 Average flux distribution in oxide-, carbide-, and metal-fueled LMFBRs

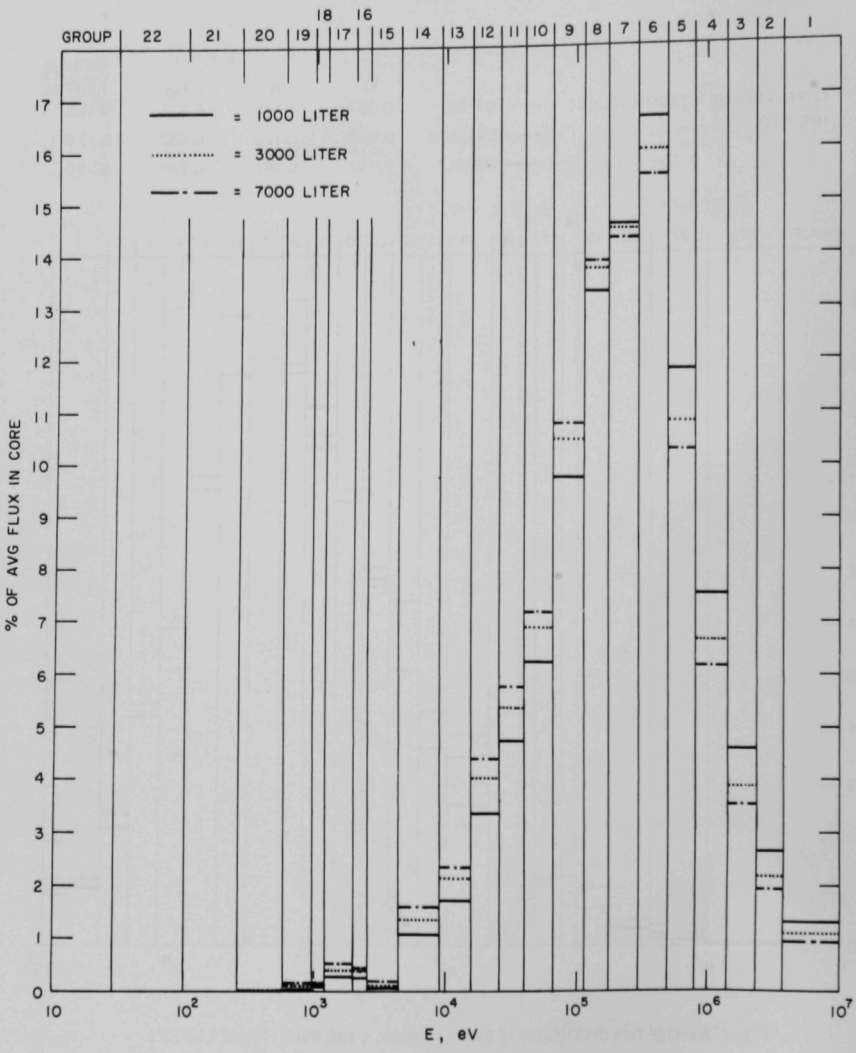

Fig. 3 Average flux distribution in spherical metal-fueled LMFBRs having volumes of 1000, 3000, and 7000 liters.
$v_f = 0.35$; $v_S = 0.20$; $v_{Na} = 0.45$

number of important neutronics parameters which will be mentioned shortly.

A nuclide is fissionable if the binding energy of the entering neutron in the compound nucleus leads to an excitation level above the fission threshold. Fission cross sections for the odd-atomic-weight nuclides U-233, U-235, and Pu-239 are shown in Fig. 4. The nuclei of these three nuclides can undergo fission after the introduction of very low energy (i.e., "thermal") neutrons, so they are characterized as "thermally fissionable" nuclides. Each of the curves shown is smoothed with regard to resonances, especially at energies below 10^4 eV, as is shown for U-235.

Figure 5 shows fission cross sections for the even-atomic-weight nuclides Th-232, U-238, and Pu-240. These curves show that the even-A nuclides have thresholds below which they do not undergo appreciable fission, and that these thresholds occur at relatively high energies. Thus, any hardening of the spectrum in a fast reactor containing one of these nuclides will result in its increased fission. Figure 5 also shows that of the three nuclides, Pu-240 has the lowest threshold for fission and highest fission cross section at a given neutron energy; it thus has the highest reactivity worth of the three.

In connection with breeding, a "fissile" nuclide is one that is thermally fissionable. A "fertile" nuclide is one that reacts with a neutron to produce directly, or by subsequent decay, a thermally fissionable nuclide. A fertile nuclide may be fissioned by high energy ($\sim$1 MeV) neutrons, but is not fissioned by thermal neutrons. The even-A nuclides Th-232, U-238, and Pu-240 are all fertile, leading to fissile U-233, Pu-239, and Pu-241, respectively.

The ratio of capture cross sections to fission cross section, denoted α, is shown in Fig. 6 for U-233, U-235, and Pu-239. It is seen that the parasitic capture cross sections fall off more rapidly with increasing energy than do the corresponding fission cross sections for U-233, U-235, and Pu-239; i.e., these nuclides are "worth" more in harder spectra. The sodium void effect discussed in Section VI-B is closely related to this parameter.

It was mentioned earlier that there are current uncertainties in certain neutronics parameters; these uncertainties are important in both safety and economic considerations in the design of large LMFBRs. The most significant parameters are α, σ_f, and ν for Pu-239, and σ_c, σ_{in}, and σ_f for U-238 (see Nomenclature for definition of symbols). Recent calculations[4] indicate that the greatest of these uncertainties, and the most important in terms of the economics of large, relatively soft-spectrum LMFBRs, is α for Pu-239 at energies below about 20 keV; next in importance appear to be ν for Pu-239 and

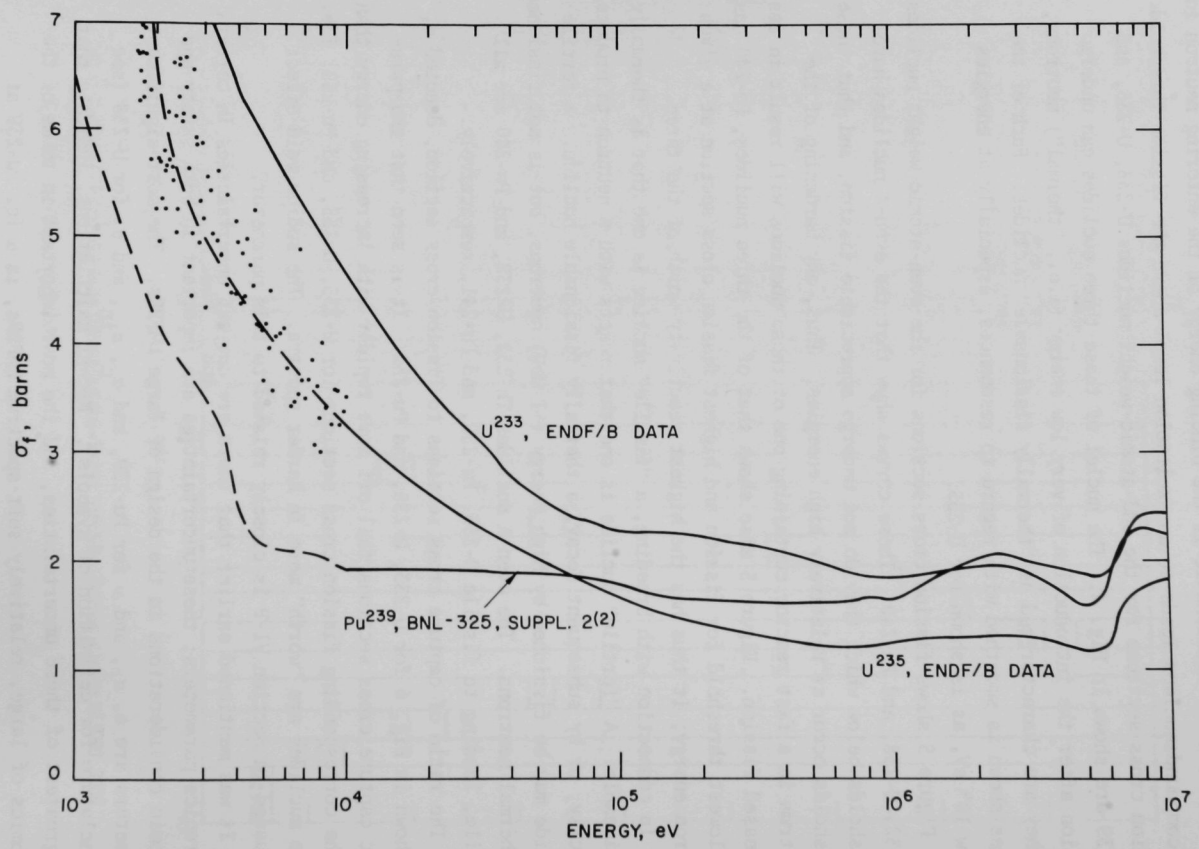

Fig. 4 Fission cross sections of odd-A nuclides

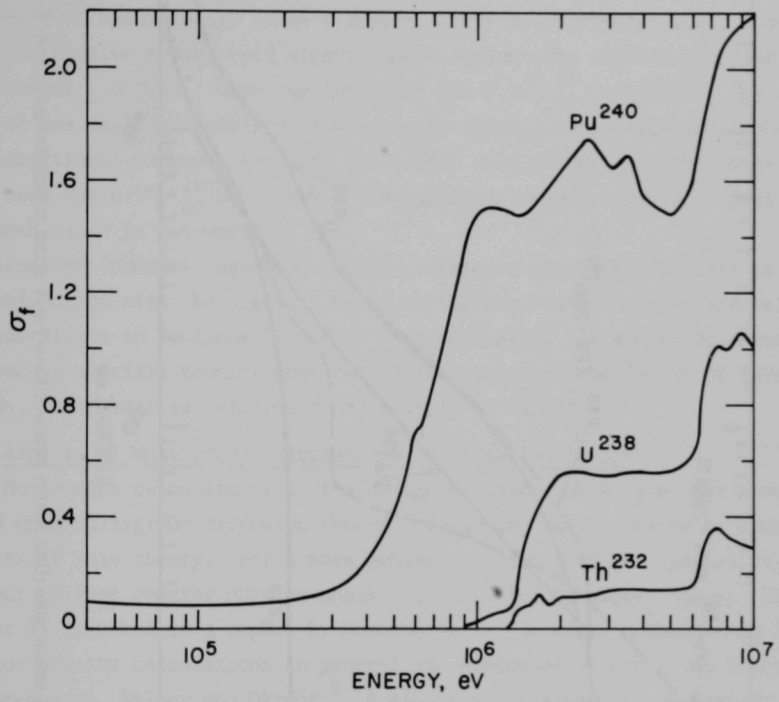

Fig. 5 Fission cross sections of even-A nuclides (ENDF/B data)

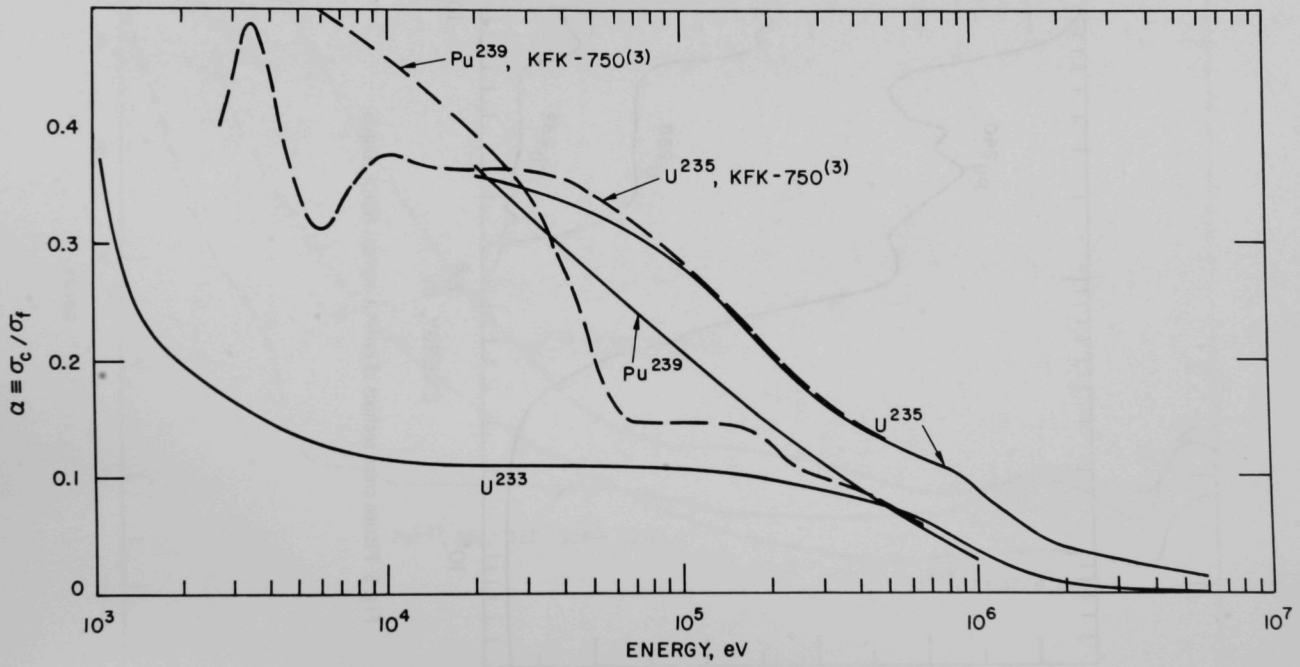

Fig. 6 Capture-to-fission cross section ratios (Data sources same as cited in Fig. 4 except dashed-line data from KFK-750[3])

σ_c for U-238. The effects of low and high values of α for Pu-239 on breeding in oxide, carbide and metal fuel LMFBRs have been discussed in a paper by Butler, et al,[5] and are given later in Table VI of this report.

Another study has reported the effect of uncertainties in nuclear parameters on the fuel costs for two oxide-fuel LMFBRs.[4] One of these reactors was designed specifically to meet severe safety requirements (i.e., a near-zero or negative sodium void effect, and a sodium-out, negative Doppler coefficient $\geq$ 0.004). Here the fuel cost was $0.70^{+.24}_{-.09}$ mills/kwh. The other reactor was designed solely on the basis of thermal-hydraulics and economics considerations, without regard to the sodium void effect. In this case the fuel cost was $0.50^{+.16}_{-.09}$ mills/kwh. The magnitude of uncertainty in fuel cost for both cases is noteworthy.

Further comments regarding nuclear parameter uncertainties will be made in conjunction with the discussions on multigroup cross sections and safety considerations in Sections II and VI, respectively. For a more detailed discussion of specific neutron physics considerations in the design of large LMFBRs, the reader is referred to an article by Okrent.[6]

II. Aspects of Multigroup Calculations in Diffusion Theory

Neutronics calculations in the design of large LMFBRs are most commonly based upon multigroup diffusion theory. Following is an outline of some aspects of this theory. For a more general treatment of the specialized subject of fast reactor physics analysis, including transport theory, the reader is referred to a report by Meneghetti.[7] Numerical methods used in reactor physics calculations in general are discussed by Clark and Hansen[8] and Greenspan, Kelber and Okrent.[9] A classical treatment of elementary reactor theory is given by Glasstone and Edlund[10] and a more basic treatment is given by Weinberg and Wigner.[11]

For a fast reactor in steady-state operation we want to determine the neutron flux per unit energy interval at space point $\vec{r}$. Given this distribution we can calculate other parameters of interest, such as the spatial variation of fission density, which determines coolant requirements throughout the reactor. The rate of type x reaction (fission, capture, etc.) of nuclide m in region V_k of the reactor is:

$$\int_{V_k} \int_{E} N^m(\vec{r}) \sigma_x^m(E) \phi(E,\vec{r}) dE dv \qquad (1)$$

In multigroup analysis the energy space is converted from a continuous to a discrete structure so that the group flux for group j ($E_{j-1} \leq E \leq E_j$) is given by:

$$\Phi_j(\vec{r}) = \int_{E_{j-1}}^{E_j} \Phi(E,\vec{r})dE \tag{2}$$

Then a group cross section, σ^m_{xj}, is defined:

$$\sigma^m_{xj} = \frac{\int_{E_{j-1}}^{E_j} \sigma^m_x(E)\Phi(E,\vec{r})dE}{\Phi_j(\vec{r})} \tag{3}$$

This parameter is commonly evaluated by assuming that the group flux is separable in energy and space, which permits the spatial component to be cancelled out. It is thus important to consider the conditions in multigroup diffusion theory under which the assumption of flux separability is valid.

Consider first a bare homogeneous reactor in a vacuum. Here diffusion theory predicts that a given group flux vanishes at a certain distance, the extrapolated end-point, beyond the physical boundary of the reactor. The extrapolated end-point actually varies with neutron energy, but here assume that it is the same for neutrons of all energies. For this special case it can be shown[11] that the flux is separable in energy and space:

$$\Phi(E,\vec{r}) = \phi(E)\cdot R(\vec{r}) \tag{4}$$

i.e.,

$$\Phi_j(\vec{r}) = R(\vec{r}) \int_{E_{j-1}}^{E_j} \phi(E)dE \equiv R(\vec{r})\phi_j \tag{5}$$

and that the spatial distribution $R(\vec{r})$ is the fundamental solution of the wave equation:

$$\nabla^2 R(\vec{r}) + B^2 R(\vec{r}) = 0 \tag{6}$$

where the eigenvalue B^2 is called the geometric buckling. For a homogeneous bare spherical reactor having $R(R_e) = 0$,

$$R(r) = (\text{const})\left(\frac{\sin Br}{r}\right) \tag{7}$$

and:

$$B^2 = \left(\frac{\pi}{R_e}\right)^2 \tag{8}$$

Similarly for a homogeneous bare cylindrical reactor having $R(\vec{r}) = \Theta(r)\cdot Z(z)$ and $\Theta(R_e) = 0$, $Z(H_e) = 0$

$$R(r,z) = (\text{const})\, J_0(B_r r) \cos B_z z \tag{9}$$

and:

$$B_r^2 = \left(\frac{2.405}{R_e}\right)^2 , \quad B_z^2 = \left(\frac{\pi}{H_e}\right)^2 \tag{10}$$

$$B^2 = B_r^2 + B_z^2 \tag{11}$$

The geometric buckling, which decreases with increasing reactor size, is a measure of neutron leakage from the reactor.

The multigroup diffusion equations will shortly be given in terms of the generalized group fluxes defined by equation (2). Using equations (5) and (6) it is readily shown that for a homogeneous bare reactor the spatial distribution of the flux cancels out leaving the multigroup equations with the set of group fluxes $[\phi_j]$ as the dependent variables. This is known as the fundamental mode treatment; it permits a complete solution of equation (5) to be obtained for this case.

For most non-annular geometry reactors the spatial and energy distribution of flux near the core center is very much like that in the equivalent bare core, especially for larger reactors where the center region is less affected by conditions near the outer surface. Thus, the average cross sections defined by equation (3) are generally evaluated from known cross section variation with energy using a large number of groups in a fundamental mode treatment; they are known as the multigroup cross sections. The averaging process is hence exact within the framework of diffusion theory to the extent that the fundamental mode flux approximates that in the real reactor, i.e., to the extent that averaging over energy space approximates averaging over energy and dimension space.

The actual technique used in cross section averaging is to have continuous σ-functions or a many-group library of cross-section variation with energy (e.g., 100 groups for the GAM-II computer code; thousands of groups for the ELMOE and MC^2 codes) which are used with one of a number of fundamental mode calculational models to generate a desired set of say, 22- or 26-group cross sections. The group structure, i.e., energy intervals, is usually selected to emphasize the region where the predominance of the flux is. Thus, a group structure that is suitable for a thermal reactor spectrum is unsuitable for a fast reactor spectrum. A representative 22-group structure is shown at the top of Figs. 2 and 3. It is frequently desirable to reduce a relatively large number of groups to a smaller number for improved speed of computation; this is especially true for a two-dimensional problem. Such a reduction is

accomplished as above; it is known as group-collapsing.

Mention was made earlier of current uncertainties in basic neutronics parameters. In the process of converting basic energy-dependent cross section data to multigroup cross section sets, further errors can arise. These latter are due to the fine-structure sensitivity of the weighting flux spectrum to relative amounts, spatial distributions, and temperature effects of nuclides present in the reactor of interest, i.e., to methods for treating resonance self-shielding and Doppler broadening in the heavy isotopes, heterogeneity, etc.

Intercomparison calculations of simple geometry fast reactors by different organizations were reported by Okrent.[12] These comparisons showed, for example, significant differences in predicted critical mass and the sodium void effect. It is thus evident that much work remains to be done with regard to the generation and evaluation of fast reactor multigroup cross section sets. Such evaluation is frequently done via analysis of zero-power critical experiments whose dimensions and compositions are similar to those of the reactor of primary interest.

We use a given set of multigroup cross sections in setting up and solving the corresponding set of multigroup diffusion equations, with the following notation for group ordering:

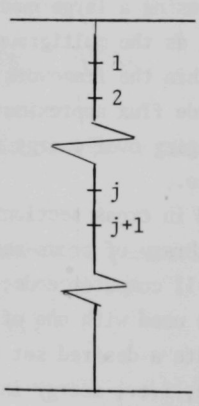

The jth group steady state diffusion equation is:

$$D_j \nabla^2 \Phi_j(\vec{r}) - \Sigma_{tj} \Phi_j(\vec{r}) + S_j = 0 \quad . \tag{12}$$

where:

$$\Sigma_{tj} = \Sigma_{cj} + \Sigma_{fj} + \sum_{k=j+1}^{j+M} \Sigma_{j\to k} \tag{13}$$

and

$$S_j = \sum_{i=j-M}^{j-1} \Sigma_{i\to j}\, \Phi_i(\vec{r}) + \frac{x_i}{k_{eff}} \sum_{i=1}^{J} (\nu\Sigma_f)_i\, \Phi_i(\vec{r}) \tag{14}$$

Note that each of the macroscopic cross sections in equations (13) and (14) is actually the sum over m nuclides:

$$\Sigma_{xj} = \sum_{m} N^m \sigma^m_{xj} \tag{15}$$

The diffusion coefficient is defined as:

$$D_j = \frac{1}{3}\left[\sum_{m} N^m \sigma^m_{tr\ j}\right]^{-1} \tag{16}$$

where for inelastic scattering assumed isotropic in the laboratory system:[7]

$$\sigma^m_{tr\ j} = \sigma^m_{cj} + \sigma^m_{fj} + \sigma^m_{in\ j} + \sigma^m_{el\ j}\,(1-\bar{\mu}) \tag{17}$$

and $\bar{\mu}$ is the average cosine of the elastic scattering angle in the laboratory coordinate system. The fission neutrons are born with approximately a Maxwellian distribution in energy, $\chi(E)$, with:

$$\chi_j = \int_{E_{j-1}}^{E_j} \chi(E)\,dE \tag{18}$$

The mean energy of a fission neutron is about 2 MeV.

The first term in the diffusion equation (12) represents jth group neutron leakage from the elemental volume at $\vec{r}$. The second term in equation (12) represents neutron loss by capture, fission and scattering out of group j. The third is the source term, and is composed of scattering into group j from M

groups above it (M is termed the downscatter band), plus those fission neutrons produced in each group that are born with energies within group j.

The usual procedure for solution of equation (12) is to make a finite difference approximation to the first term, then apply appropriate boundary conditions on the closed surface surrounding the system, and flux and current continuity conditions at internal interfaces between regions of different composition. The resulting set of difference equations may be written in matrix notation:[13,7]

$$[M][\Phi] = 0 \tag{19}$$

The matrix $[M]$ contains neutron production and loss terms, and the column matrix $[\Phi]$ is made up of the group fluxes. With $[M^+]$ the transpose of $[M]$,

$$[M^+][\Phi^+] = 0 \tag{20}$$

defines the adjoint group fluxes Φ_j^+. An important use of these latter is in perturbation analysis.[7]

Expressing $[M]$ as the sum of a production matrix $[P]$ and a loss matrix $[L]$, the stationary system is conventionally defined as:

$$\left\{-[L] + \frac{1}{k}[P]\right\}[\Phi] = 0 \tag{21}$$

Rearranging,

$$[L]^{-1}[P][\Phi] = k[\Phi] \tag{22}$$

Thus solutions $[\Phi]_i$ exist for values of k equal to the eigenvalues of the matrix $[L]^{-1}[P]$. The largest eigenvalue is identified as k-effective (or k_{eff}), and the associated $[\Phi]$is the desired stationary solution for the neutron flux. Obtaining the $[\Phi]$vector in complex situations can be very difficult, and is the subject of intensive study, even up to the present time.

In principle, if one has available a true three-dimensional diffusion-theory computer code, the foregoing generalized procedure can be used to analyze any reactor configuration without concern for flux separability. These codes are very complex, and require of a computer great speed of calculation and large rapid-access storage capacity. Hence development of true three-dimensional diffusion theory codes has been undertaken only rather recently. There are, however, a number of two-dimensional diffusion theory codes currently in use. Such codes can treat a fully reflected

multiregion cylindrical reactor in (r,z) coordinates without concern for flux separability, if the reactor is θ-symmetric. Most fast reactors, except those of a modular design, are to a good first approximation θ-symmetric, and thus can be closely represented in a two-dimensional (r,z) calculation. If a two-dimensional code is used in (r,θ) or (x,y) coordinates, the former, for example, to study one module of a modular reactor and the latter to study local effects around a control rod, then the problem of describing the z-component of the flux arises. This is commonly done by assuming separability with regard to the z-component, i.e., in cylindrical coordinates,

$$\phi_j(\vec{r}) = Z(z) \int_{E_{j-1}}^{E_j} \phi(E,r,\theta)dE \tag{23}$$

where, for $Z(H_e) = 0$,

$$B_z^2 = \left(\frac{\pi}{H_e}\right)^2 \tag{24}$$

Under the present state of the digital computer art, two-dimensional multigroup diffusion calculations are rather time-consuming if more than a few flux groups and more than a modest number of spatial mesh points are required. Moreover, models based upon one-dimensional codes can be made to describe rather well the behavior of even small, fully reflected fast reactors. Thus, the great majority of multigroup diffusion calculations are currently made, and probably will continue to be made for some time, using one-dimensional codes.

If a θ-symmetrical reactor contains one or more radial core regions of enrichment and is surrounded by a lateral reflector, but is bare on the top and bottom (i.e., has a z-directional buckling that is constant over all groups and regions), then:

$$\phi(E,\vec{r}) = \phi(E,r)\cdot Z(z) \tag{25}$$

and

$$\phi_j(\vec{r}) = Z(z) \int_{E_{j-1}}^{E_j} \phi(E,r)dE = Z(z)\phi_j(r) \tag{26}$$

If the reactor is also z-symmetric and $Z(H_e) = 0$,

$$Z(z) = (\text{const}) \cos \frac{B_z z}{2} \tag{27}$$

where:

$$B_z^2 = \left(\frac{\pi}{H_e}\right)^2 \tag{28}$$

Equation (27) shows the "chopped cosine" behavior of the flux in the z-direction in a cylindrical reactor. This description is exact only in a reactor that is bare on the top and bottom, where the separability of equation (25) applies.

By substituting equation (26) into equation (12) it can be shown that the set of multigroup diffusion equations becomes one dimensional in the group fluxes $[\phi_j(r)]$, with the z-component satisfying:

$$\frac{1}{Z}\frac{d^2Z}{dz^2} = B_z^2 \tag{29}$$

That is, the transverse neutron leakage per unit volume at r in this case is converted into an equivalent absorption term:

$$D_j B_z^2 \phi_j(r) = \Sigma_{aj}\phi_j(r) \tag{30}$$

which is added to the second term of equation (12). A reactor that is reflected on the top and bottom, but is laterally bare, is treated in a parallel manner.

A number of versatile computer codes are available for solving the one-dimensional multigroup diffusion equations where transverse leakage is treated as above; MACH 1 is such a code.[14] In order to see how these codes can be used to obtain an approximate description of the behavior of a fully reflected reactor, where, in principle, flux is inseparable in energy and space, we employ the notion of "reflector savings." Consider a fully reflected cylindrical reactor that is just critical. If the lateral reflector is removed, increased neutron leakage causes the reactor to go sub-critical. The increase in core radius required to make the reactor just critical is the radial reflector savings. The axial reflector savings is defined analogously.

One model that is used to analyze fully reflected fast reactors using group-independent transverse bucklings is called self-consistent diffusion

theory.[15] There are a number of alternate ways in which this analysis can be carried out, all of them of an iterative nature. Basically, it consists of determining the core composition for which the radial reflector savings in slab geometry (z-direction calculation) and axial reflector savings in cylindrical geometry (r-direction calculation) give the same total leakage as that from a bare core having the same composition. Equations (10) and (11) are fundamental to the method.

The use of group-independent transverse bucklings in multigroup diffusion calculations can be shown to be mathematically sound,[14] but requires that the group fluxes all have the same shape and extrapolated end-point. The extrapolated end-point is, however, not the same for all groups. Thus, an alternate approach is to use group-dependent bucklings in the iterations. It is argued that these give better representation of the individual group flux spatial variations, and thus, better predictions of leakage. At this point it can only be said that the superiority of one of these methods to the other depends strongly on which neutronics parameter one is attempting to compute, as well as on the reactor geometry and size.

The core of a large LMFBR contains at least two regions of radially different enrichment, as will be discussed further in Section IV. Using multigroup notation, consider the power distribution in a multiregion core. The fission power density at point $\vec{r}$ in region $\underline{k}$ is:

$$P_k(\vec{r}) = (\text{const}) \sum_j \left[\sum_m N_k^m \sigma_{fj}^m \right] \phi_{kj}(\vec{r}) \qquad (31)$$

The total power in region k is:

$$Q_k = \int_{V_k} P_k(\vec{r}) dV \qquad (32)$$

and the average power density in region $\underline{k}$ is:

$$\overline{P}_k = \frac{1}{V_k} \int_{V_k} P_k(\vec{r}) dV = \frac{\text{const}}{V_k} \sum_j \left[\sum_m N_k^m \sigma_{fj}^m \right] \int_{V_k} \phi_{kj}(\vec{r}) dV \qquad (33)$$

If the maximum power density occurs at $\vec{r}_0$ in region $\underline{s}$ of the core, then the core maximum-to-average power density is:

$$\frac{P_{max}(\vec{r}_0)}{\overline{P}_{core}} = \frac{\sum_j \left[\sum_m N_s^m \sigma_{fj}^m \right] \phi_{sj}(\vec{r}_0)}{\frac{1}{V_{core}} \sum_{core\ k's} \left\{ \sum_j \left[\sum_m N_k^m \sigma_{fj}^m \right] \int_{V_k} \phi_{kj}(\vec{r}) dV \right\}} \quad (34)$$

The overall maximum-to-average core power density can be rigorously separated into a radial and a z-directional or axial component if equation (26) applies, i.e., the reactor is bare on the top and bottom. If, in addition, equation (27) applies, i.e., the reactor is also z-symmetric, the maximum power density occurs at the reactor midplane. Then:

$$\frac{P_{max}(r_0,0)}{\overline{P}_{core}} = \left(\frac{P_{max}}{\overline{P}_{avg}}\right)_{ax} \cdot \left(\frac{P_{max}}{\overline{P}_{avg}}\right)_{rad} \quad (35)$$

where:

$$\left(\frac{P_{max}}{\overline{P}_{avg}}\right)_{ax} = \frac{Z(0)}{\frac{1}{H_e} \int_{-H_e/2}^{H_e/2} Z(z)dz} \quad (36)$$

and:

$$\left(\frac{P_{max}}{\overline{P}_{avg}}\right)_{rad} = \frac{\sum_j \left[\sum_m N_s^m \sigma_{fj}^m \right] \phi_{sj}(r_0)}{\frac{1}{\pi R_{core}^2} \sum_{core\ k's} \left\{ \sum_j \left[\sum_m N_k^m \sigma_{fj}^m \right] \int_{r_k} \phi_{kj}(r) \cdot 2\pi r dr \right\}} \quad (37)$$

The above separability holds rather well for the cores of most LMFBRs (even for EBR-II, whose core volume is under 100 liters).

III. Breeding

The nuclear reactions significant to breeding in the U-Pu breeding cycle are:

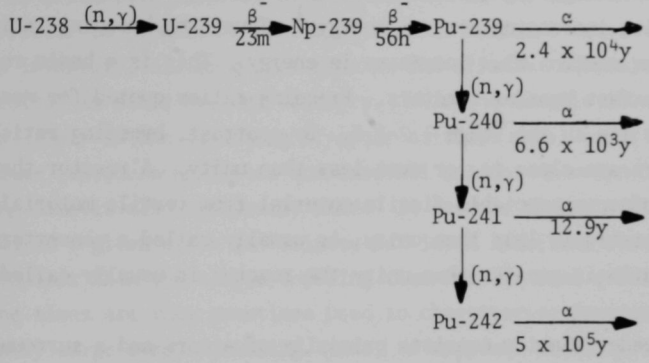

In general terms, breeding is the process of converting a fertile nuclide to a fissile nuclide, e.g., U-238 to Pu-239 and Pu-240 to Pu-241, as shown above.

The breeding ratio is defined in several ways, the commonest being on a point-in-time basis:

$$BR = \frac{\text{fertile capture rate over reactor}}{\text{fissile absorption rate over reactor}} = \frac{\text{rate of formation of fissile}}{\text{rate of consumption of fissile}} \quad (3$$

Thus, from equation (1),

$$BR = \frac{\int_{E,V} \left[N^{238}(\vec{r})\sigma_c^{238}(E) + N^{240}(\vec{r})\sigma_c^{240}(E) \right] \Phi(E,\vec{r})\,dE\,dV}{\int_{E,V} \left[N^{239}(\vec{r})\sigma_a^{239}(E) + N^{241}(\vec{r})\sigma_a^{241}(E) \right] \Phi(E,\vec{r})\,dE\,dV} \quad (39)$$

here neglecting effects of isotopes above Pu-241. The breeding ratio can also be defined in terms of suitable averages of α and ν for the fissile material and ν' for the fertile material:[6]

$$BR = \frac{\nu - 1 - \alpha - C - L + (\nu' - 1)F}{1 + \alpha} \quad (40)$$

The numerator of equation (40) is proportional to the rate of production of excess neutrons for breeding. The C and L terms represent neutron loss by parasitic absorption and leakage, respectively, and the $(\nu' - 1)$ F term represents the fast fission bonus due to the fertile material.

As was shown in Fig. 6, $\underline{\alpha}$ for the fissile nuclides decreases with increasing neutron energy. The average number of neutrons emitted per fission, $\underline{\nu}$, increases with increasing neutron energy.[1] Thus, the breeding ratio increases as the neutron flux increases in energy. This is a basic reason for interest in fast breeder reactors. Breeding ratios quoted for most 1000 MWe LMFBRs lie in the range 1.2-1.5. By contrast, breeding ratios for thermal breeders are close to, or even less than unity. A reactor that is designed to produce appreciable fissile material from fertile material, but whose breeding ratio is less than unity, is usually called a converter. If the breeding ratio is greater than unity the reactor is usually called a breeder.

A fast breeder reactor consists primarily of a core and a surrounding blanket. The core is fueled with a mixture of uranium and plutonium oxides, carbides, or alloys of the metals. In a large core, say 6000 liters, the average fissile plutonium enrichment $([N^{239}+N^{241}]/[N^{238}+N^{239}+N^{240}+N^{241}+N^{fp}])$ is about 0.12-0.15. There is thus a relatively large amount of U-238 in the core, i.e., depending upon the reactor configuration and composition, about 60% of the total breeding occurs in the core.

The blanket is fueled with uranium oxide, carbide, or metal, that initially contains little fissile material (except in certain cases of initial startup). The blanket is designed to absorb most of the neutrons that leak from the core. Only about 10-15% of the total reactor power is generated in the blanket during an equilibrium operating cycle (see Section V), hence its coolant volume fraction can be made smaller and its fuel volume fraction made larger than the corresponding core volume fractions; this enhances neutron capture in the blanket. If the blanket is made too thin, excessive neutron loss by leakage will occur, even if the blanket is surrounded by a reflector. If the blanket is made too thick, the additional fabrication required, as well as the additional reprocessing to recover its fissile material becomes too costly. An economic balance is thus involved in optimum blanket design.[16] This balance includes such details of the fuel cycle as the fraction of the core and blanket elements that are replaced at the end of each operating cycle, and whether and how the remaining elements are relocated or "shuffled."

It is not difficult to design two reactors that have the same breeding ratio but different critical masses. Everything else being equal (but not defined here) the reactor having the smaller fissile inventory would be preferable. Thus, a more general figure of merit must depend both upon breeding ratio and critical mass; the doubling time is such a figure of merit. The simple or arithmetic doubling time is defined as the time in years required for a breeder to produce an excess of fissile material equal to its original fissile inventory, assuming that none of the fissile material produced is "reinvested" in other breeder reactors. Here the fissile inventory can be defined simply as the beginning-of-cycle critical mass, or it can be defined to include reprocessing losses and external holdup. A compound or geometric doubling time is also frequently used. It assumes that the fissile material produced in a given cycle is "reinvested" in an identical breeder, and hence it is smaller than the simple doubling time for the same reactor. Compound doubling times are thus sometimes used to characterize reactors that have inherently large simple doubling times. A compound doubling time is meaningful only for a power reactor network containing a number of breeder reactors having similar breeding characteristics.

The doubling time, suitably defined, gives a measure of the fuel cycle cost for a breeder reactor. The most important figure of merit, however, is the actual mills per kilowatt hour. But different organizations use different techniques of cost analysis, some involving proprietary cost information, and hence comparisons on a true cost basis are difficult.

The simple doubling time is derived as follows, neglecting reprocessing losses and external inventory (quantities in parentheses are rates):

$$BG \equiv BR - 1 = \frac{(\text{fert caps})}{(\text{fiss absns})} - 1 = \frac{(\text{fert caps}) - (\text{fiss absns})}{(\text{fiss absns})}$$

$$= \frac{(\text{fiss gain})}{(\text{fiss absns})} \qquad (41)$$

Using a one-group average cross-section formalism:

$$\frac{\text{(fiss absns)}}{\text{(fissions)}} \simeq \frac{N^{239}\left(\overline{\sigma_f^{239}} + \overline{\sigma_c^{239}}\right) + N^{241}\left(\overline{\sigma_f^{241}} + \overline{\sigma_c^{241}}\right)}{N^{239}\,\overline{\sigma_f^{239}} + N^{241}\overline{\sigma_f^{241}}}$$

$$= 1 + \frac{\overline{\sigma_c^{239}} + (N^{241}/N^{239})\ \overline{\sigma_c^{241}}}{\overline{\sigma_f^{239}} + (N^{241}/N^{239})\ \overline{\sigma_f^{241}}} = 1 + \bar{\alpha} \qquad (42)$$

where $\bar{\alpha}$ is a suitably averaged capture-to-fission ratio for the thermally fissionable isotopes. Thus:

$$\text{(fiss gain)} = BG(\text{fiss absns}) = BG(1 + \bar{\alpha})\ \text{(fissions)} \qquad (43)$$

But:

$$\text{(fiss gain)} = \frac{\text{kg fiss matl gained}}{\text{yr}} \times \frac{10^3\ \text{gms}}{\text{kg}}$$

$$\times \frac{\text{mole}}{239\ \text{gms}} \times \frac{6.02 \times 10^{23}\ \text{atoms}}{\text{mole}} \qquad (44)$$

$$\text{(fissions)} = P \times (1 - F) \times \frac{365\varepsilon\ \text{days}}{\text{yr}} \times \frac{10^6\ \text{watts}}{\text{MW}}$$

$$\times \frac{2.91 \times 10^{10}\ \text{fiss}}{\text{watt sec}} \times \frac{3600\ \text{sec}}{\text{hr}} \times \frac{24\ \text{hrs}}{\text{day}} \qquad (45)$$

(Here, P = total reactor power, MW; F = fraction of fissions in U-238 and Pu-240; ε = fraction of time reactor is at full power.) Hence:

$$\frac{\text{kg fiss matl gained}}{\text{yr}} = 0.3643\ BG(1 + \bar{\alpha})\ (1 - F)\ P\varepsilon \qquad (46)$$

With the core critical mass denoted as M_c, the doubling time is given by:

$$DT = \frac{M_c}{\text{kg fiss matl gained/yr}} = \frac{2.74\ M_c}{BG(1 + \bar{\alpha})(1 - F)\ P\varepsilon} \qquad (47)$$

The shorter the doubling time of a breeder, the better its performance, other things being equal. For large fast breeders, $\bar{\alpha} \simeq 0.2$, $F \simeq 0.2$, and $\varepsilon \simeq 0.8$. Thus:

$$DT \simeq \frac{3.57\ M_c}{(BG)(P)} \qquad (48)$$

If M_c = 2100 kg, P = 2500 MW, and BG = 0.3, then:

$$DT \simeq \frac{3.57 \times 2100}{0.3 \times 2500} = 10.0 \text{ yrs}$$

For perspective, the doubling time for electrical power in the U.S. is about 8-10 years.

Another parameter of interest is the specific power, P_s:

$$P_s = P/M_c \tag{49}$$

The reciprocal of the specific power, the specific inventory, is also commonly employed. As is seen from the definition of the doubling time, the higher the value of the specific power, the more efficient the reactor is in terms of breeding. Generally, LMFBRs have specific powers in the range 900-1400 kw/kg of fissile plutonium. For comparison, water-cooled thermal reactors have specific powers in the range 1000-1500 kw/kg of fissile uranium plus plutonium, with boiling water reactors near the lower end and pressurized water reactors near the upper end.[17] An important use of specific power is in translating future electrical power requirements into equivalent fissile material requirements, and thus into U_3O_8 requirements for various potential combinations of thermal, converter, and breeder reactors.

If the fissile enrichment is uniform over the core of an LMFBR, then the conversion ratio for the core is defined analogously to the breeding ratio for the reactor:

$$CR = \frac{\text{fertile capture rate over core}}{\text{fissile absorption rate over core}} \tag{50}$$

If the core contains more than one zone of enrichment, a conversion ratio is defined as above for each zone. In this case, an overall core conversion ratio may be defined in different ways, e.g., on the basis of volume weighting of individual zone conversion ratios. Since the numerator of equation (50) is approximately proportional to the U-238 atom density and the denominator to the Pu-239 atom density, the conversion ratio decreases with increasing enrichment. If it is desired to increase the coolant volume fraction in a given core, the fuel volume fraction must usually be decreased. When this is done, the fuel that is in the core must have a higher fissile content and, therefore, the conversion ratio is decreased.

The conversion ratio is a key parameter in evaluating the behavior of a fast power breeder during the operating time between loadings. The value of

the conversion ratio depends strongly on the specific core design, and varies from ∿0.6 to 1.1. To see the significance of the conversion ratio, consider two reactors, one having CR < 1, and the other having CR > 1, as shown in Fig. 7. A conversion ratio that is less than 1.0 means that fissile material in the core is depleted more rapidly than it is replaced. This results in a net effective movement of fissile material away from the core center (including the buildup in the blankets) and, together with fission product buildup, causes a reactivity decrease with time. Thus, control rods must be withdrawn for compensation during the operating cycle. For a conversion ratio sufficiently greater than 1.0, the opposite is true, and the control rods must be inserted further with time.

IV. Radial Core Zoning

A fuel element is designed to operate at a certain maximum power density to a specified burnup. These operating limitations are determined by heat transfer and fluid flow, materials properties, mechanical design, and safety considerations. If all the fuel elements in the core of a large LMFBR have the same enrichment, those at the center will be exposed to the highest flux and operate at the highest power density. In addition, if all the elements are replaced at the end of an operating cycle, those in the center will have the highest burnup. In such a reactor the radial maximum-to-average power density would be about 1.7, i.e., the average midplane power density and burnup would only be about 1/1.7 of the corresponding core-center values.

Radial zoning of core enrichment is used to reduce the radial maximum-to-average power density. This permits more of the elements to be operated at higher power densities and to higher burnups. The former leads directly to a higher reactor power and the latter to reduced unit energy cost. In the case of a 1000 MWe LMFBR, the core is usually divided into two zones (although as many as five zones have been considered), the elements of the outer zone being enriched more than those of the inner zone. This results in a radial maximum-to-average core power density of about 1.23 if the core height-to-diameter ratio is about 0.4. Under these conditions, the axial maximum-to-average core power density is also about 1.23, and the overall core maximum-to-average value is about 1.5.

The $(P_{max}/P_{avg})_{radial}$ for the zoned core is actually a function of two variables: the distribution of core volume between the two zones, and the relative enrichments in each of them. The minimum $(P_{max}/P_{avg})_{radial}$ occurs approximately at the enrichment ratio that produces equal maximum power

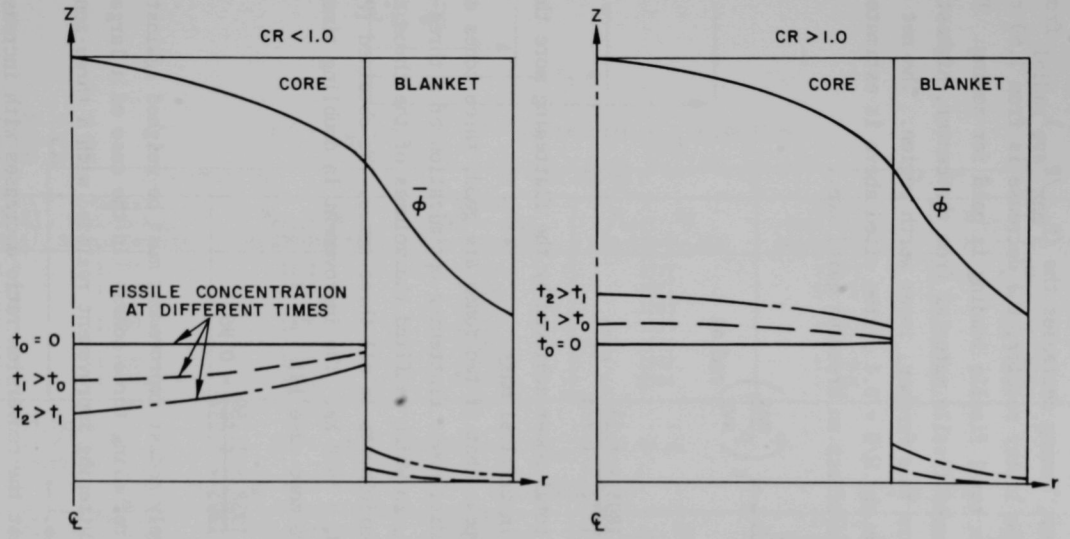

Fig. 7 Effect of conversion ratio on fissile concentration as a function of operating time

densities in the two zones when these zones are made equal in volume. Table I shows calculations in which both relative volumes and enrichments were varied for one reactor having H/D = 0.4 and another having H/D = 0.8. In the case of the former reactor, zoning decreases the $(P_{max}/P_{avg})_{radial}$ from 1.77 to 1.23; in the case of the latter reactor, the decrease is from 1.69 to 1.20.

A penalty in total fissile loading is paid for zoning. This is simply because zoning moves fissile material from the center, highest reactivity worth region of the core to a farther, lower worth region. The net effect on doubling time for the H/D = 0.4 system cited above is estimated, noting that zoning has little effect on breeding gain; i.e.,

$$DT \propto \frac{M_c}{\bar{P}} \propto M_c \left(\frac{P_{max}}{P_{avg}}\right)_{radial}$$

Thus:

$$\frac{DT_2}{DT_1} = \frac{1893 \times 1.234}{1772 \times 1.773} = 0.74$$

Here the higher total power achieved by the flattening more than compensates for the penalty in critical mass.

It would appear that if two zones are good, three zones are better. We did a partial radial power flattening optimization of a three-zone core for a 1000 MWe reactor, in which we fixed the volumes of the three zones as equal, but varied the enrichments in all three zones. We obtained $(P_{max}/P_{avg})_{radial}$ = 1.159 for an M_c = 1938 kg. The improvement in doubling time over the corresponding two-zone case is:

$$\frac{DT_3}{DT_2} = \frac{1938 \times 1.159}{1893 \times 1.234} = 0.96$$

Here the relatively modest improvement must be weighed against the significant complication of refueling three zones. In the case of a larger LMFBR, say 2000 MWe, the flattening improvement realized with a three-zone core may make it most desirable.

We noted that the conversion ratio decreases with increasing enrichment. Since the enrichment is lower in the inner zone of a two-zone core, it has a higher conversion ratio. Typical values are CR_i = 0.9; CR_o = 0.6. This implies that during the course of an operating cycle, fissile material is depleted more rapidly from the outer zone than from the inner zone; i.e., there

TABLE I. Two-zone-core Results, Oxide Fuel Reactor

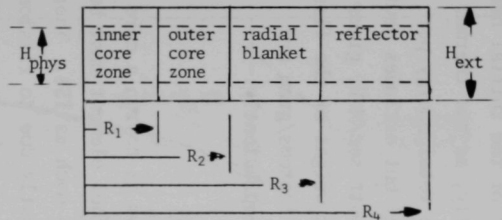

R_2 = 130.76 cm
R_3 = 168.86 cm
R_4 = 183.86 cm

H/D = $H_{phys}/2R_2$ = 0.4, $\bar{P}$ = 400 kW/liter, H_{ext} = 146.41 cm

	R_1 = 109.62 cm		R_1 = 88.185 cm		R_1 = 66.203 cm	
$\left\{\frac{N_{Pu,o}}{N_{Pu,i}}\right\}$	Radial Peak-to-Avg. Source Density	M_{crit}, Kg (Pu-239+Pu-241)	Radial Peak-to-Avg. Source Density	M_{crit}, Kg (Pu-239+Pu-241)	Radial Peak-to-Avg. Source Density	M_{crit}, Kg (Pu-239+Pu-241)
1.0	1.773	1772	1.773	1772	1.773	1772
1.1	1.684	1810	1.558	1822	1.471	1813
1.2	---	---	1.357	1863	---	---
1.3	1.499	1879	→ 1.234	1893	1.332	1860
1.4	---	---	1.286	1916	---	---
1.5	1.309	1937	1.329	1931	1.336	1879
1.7	1.277	1981	1.403	1944	1.358	1883

R_2 = 103.79 cm
R_3 = 141.89 cm
R_4 = 156.89 cm

H/D = 0.8, $\bar{P}$ = 400 kW/liter, H_{ext} = 207.09 cm

	R_1 = 89.44 cm		R_1 = 74.96 cm		R_1 = 60.30 cm	
$\left\{\frac{N_{Pu,o}}{N_{Pu,i}}\right\}$	Radial Peak-to-Avg. Source Density	M_{crit}, Kg (Pu-239+Pu-241)	Radial Peak-to-Avg. Source Density	M_{crit}, Kg (Pu-239+Pu-241)	Radial Peak-to-Avg. Source Density	M_{crit}, Kg (Pu-239+Pu-241)
1.0	1.690	1679	1.690	1679	1.690	1679
1.1	1.633	1709	1.559	1723	1.494	1721
1.3	1.517	1766	1.315	1794	1.285	1780
1.4	1.459	1792	1.204	1827	---	---
1.5	1.402	1817	1.257	1845	1.323	1815
1.6	1.344	1840	---	---	---	---
1.7	1.288	1861	1.351	1880	1.347	1835
1.8	1.232	1881	---	---	---	---
1.9	1.297	1899	---	---	---	---

is a net effective movement of fissile material toward the center of the core. This works against the basic purpose of zoning, and hence the $(P_{max}/P_{avg})_{radial}$ increases over the cycle. The resulting radial power shift must be considered in the design of a real power breeder. One method for reducing this shift is to use radial zoning of shim control; i.e., place the beginning-of-cycle hold-down control mainly in the outer core region.

The radial flux and fission density distribution for the reactor noted with the arrow in Table I is shown in Fig. 8. Also shown is the radial variation of flux shape with flux group.

V. Time-Dependent Behavior, Refueling

Fuel burnup is expressed directly as the fraction of the initial heavy atoms (U + Pu isotopes) that are burned, or equivalently, as the thermal energy released per initial mass of heavy atoms. Taking the total energy per fission as 215 MeV (which includes capture gamma energy but excludes neutrino energy), and the conversion factor as 1.5984×10^{-13} watt sec/MeV, gives 2.910×10^{10} fissions/watt sec. If the average atomic weight of the fissioned isotopes is taken equal to that of Pu-239, 2.520×10^{21} atoms/gram are destroyed. This gives 0.9977 gram fissioned/MWd, or equivalently:

$$\frac{100{,}000 \text{ MWd}}{\text{initial metric ton}} = 10.0\% \text{ burnup}$$

A major goal of the LMFBR fuel development program is to run a core loading to about 10% average burnup. To achieve this, a fuel element must be designed to operate reliably to a maximum burnup of as much as 15%. There are a number of problems in achieving such high burnup, mostly due to fission product formation. If the material is made rather porous, the gaseous fission products diffuse out of it to a great extent, and must either be contained by the cladding (non-vented element), or be allowed to leave the element (vented element). If the fuel material is not sufficiently porous, the gaseous fission products build up and cause swelling. In either case, further swelling is caused by condensed-phase fission products. If the swelling fuel has sufficient operating-temperature strength, when it contacts the cladding it will cause it to strain and ultimately fail. Fuel materials are frequently loaded into elements at 70-90% of theoretical density to accommodate swelling. However, this reduced density is deleterious both in terms of breeding and of power rating.

Even if a fuel material does not damage the cladding mechanically, it may interact with it chemically. If carbon-rich mixed carbide fuel is used in an

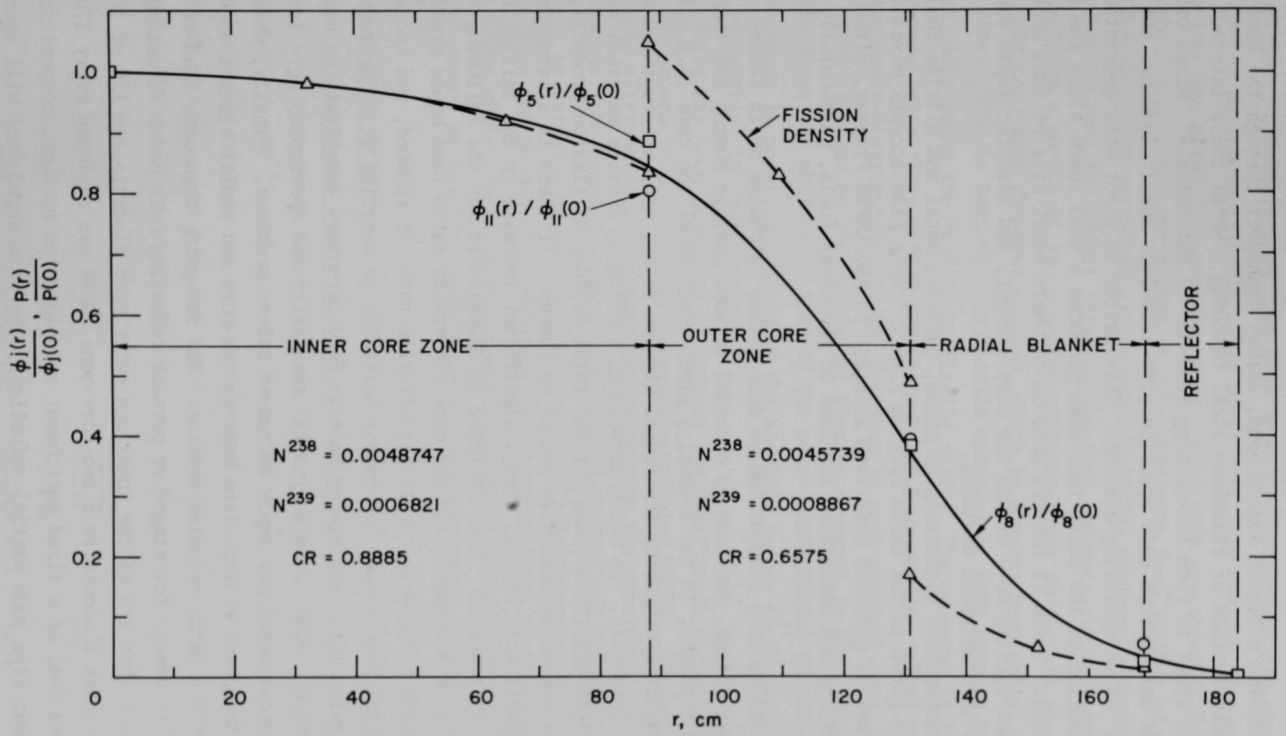

Fig. 8 Radial flux and fission density distribution in two-core-zone oxide fuel reactor

element having a liquid sodium bond, carbon transport through the bond may cause carburization of stainless steel cladding. Metal fuels interact with stainless steel to form low-melting (650-850°C) eutectics.[18] Mixed oxide fuel does not undergo such reaction with stainless steel cladding, but tends to "core" in an operating element. This latter is a not well understood redistribution of the oxide fuel that produces a void space along the axis of the element. There is concern here as to where small bits of fuel broken off in thermal cycling move within the core element, and also for rapid fuel movement in a meltdown accident.

A comparative discussion of oxide, carbide, metal and nitride fuel for LMFBRs is given in the LMFBR Program Plan.[19] This plan accepts mixed-oxide as the fuel of greatest near-term interest to the LMFBR Program, although it indicates certain attractive features of the other fuels, particularly the carbides.

Refueling of a reactor can be done either batchwise or in stages. In the former method, the core is operated to some average burnup and then is entirely replaced; in the latter, a given fraction of the core (e.g., 1/3) and a smaller fraction of the radial blanket (e.g., 1/6) are replaced at more frequent intervals. In batch refueling, sufficient fissile material must be present initially to account for the total buildup of fission products, as well as whatever depletion is caused by burnup. If there is a large decrease in reactivity with burnup, then a significant increase in the initial fissile material is required. This increase is undesirable for the following reasons. It results in a reduction in the core conversion ratio (and hence breeding ratio), both because the fertile-to-fissile ratio is reduced, and because more control poison must be present initially to override it. The reduction in conversion ratio and higher initial feed inventory constitute an economic disadvantage. Also, a large initial reactivity and correspondingly large control requirement may imply increased safety problems. Finally, shifts with time of the power distribution between the core and radial blanket are more severe with a batch-refueled reactor. The foregoing arguments lead to a general preference for staged or partial refueling over batch refueling.

Assume that 1/3 of the inner and outer core elements and 1/6 of the radial blanket elements in a two-core-zone LMFBR are replaced every 170 days, using feed fuel of a fixed enrichment and plutonium isotopic composition. After about five such partial refuelings, the discharged fuel will approach equilibrium with regard to discharge enrichment and plutonium isotopic

composition. Computer codes have been developed to predict the characteristics of an LMFBR during equilibrium cycle operation. The results of a calculation for a 1000 MWe metal fuel reactor using such a code are shown in Table II. Here the ratio of the enrichment of the outer core feed to that of the inner core feed has been varied to give a minimum radial maximum-to-average power distribution, and the oldest third of the fuel elements are replaced when they have reached a burnup of 9%, averaged over both core zones. It is seen that the inner core zone conversion ratio, which is greater than unity, decreases with time. This is because more fissile material is made than is used in this region, decreasing the fertile-to-fissile ratio. The converse is true in the outer core zone. This effect also causes the increase in radial maximum-to-average power distribution and the decrease in core critical mass, the latter also being affected by the buildup of fissile material in the blanket. Table II also shows the shift with time of the power distribution in the reactor. The increase in power generation in the blankets is due to the buildup of fissile material in these regions.

Little has been published to date on the "best" mode of initial startup (i.e., approach to equilibrium) of a stage-refueled LMFBR. There are a number of alternative modes, each depending upon the specific goal sought. For example, the reactor loading upon initial startup and subsequent refuelings may be established to give the most rapid possible approach to equilibrium. This can be done by simulating the stage loadings at the start of an equilibrium cycle, taking into account differences between the two situations, such as amount of fission products and average plutonium isotopic compositions.

VI. Reactivity Effects

A. Reactor and Kinetics and Fast Reactor Accident Considerations

Fission reactions produce neutrons by means of two mechanisms: the prompt (within $\sim 10^{-14}$ sec) emission during the fission process itself; and the emission of neutrons by certain radioactive fission products over a period of minutes. Let β be the fraction of the fission neutrons that are delayed. Its value for pertinent isotopes is given below:

Isotope	β	Isotope	β
Th-232	.022	U-238	.0157
U-233	.0027	Pu-239	.0021
U-235	.0065	Pu-240	.0026

TABLE II. Equilibrium Cycle Parameters -- 1000 MWe Metal Fuel Reactor

Parameter	Beginning-of-Life	Midlife	End-of-Life
$\left(\frac{\text{Pu-239+Pu-241}}{\text{U + Pu + FP}}\right)_i \Big/ \left(\frac{\text{Pu-239+Pu-241}}{\text{U + Pu + FP}}\right)_o$	.08963/.11990	.09084/.11718	.09157/.11470
$(CR)_i/(CR)_o$	1.106/.790	1.069/.799	1.040/.807
$\overline{CR}$	.956	.945	.935
$(P_{max}/P_{avg})_{radial}$	1.213	1.222	1.265
$\overline{(\text{Pu-239})}_o/\overline{(\text{Pu-239})}_i$	1.328	1.277	1.238
% power in inner core	47.41	47.45	47.32
% power in outer core	42.22	40.14	38.32
% power in radial blanket	5.07	5.63	6.15
% power in axial blanket	5.31	6.78	8.22
core critical mass, kg (Pu-239 + Pu-241)	1463	1452	1439

subscript i = inner core zone, o = outer core zone

Reactor specifications:

Core: H = 91.44 cm; D = 228.6 cm

v_f = 0.36

v_s = 0.20

v_{Na} = 0.44

Radial blanket: thickness = 30.48 cm

v_f = 0.48

v_s = 0.18

v_{Na} = 0.34

Axial blanket: thickness = 38.10 cm

Reflector: thickness = 15.24 cm

v_s = 0.70

v_{Na} = 0.30

If a reactor contains more than one of the above isotopes, the effective β, β_{eff}, will depend upon the relative amounts of the fissioning species and the flux distribution in energy and space. If a hypothetical step amount of reactivity less than β_{eff} is added to a reactor operating at $k_{eff} = 1.0$ at time zero, then the delayed neutrons largely determine the multiplication rate, i.e., the reactor is sub-prompt critical. If the step reactivity addition is greater than β_{eff}, the reactor will go super-critical on prompt neutrons alone, and its multiplication rate is approximately:

$$\phi(t)/\phi(o) = e^{t/T} \tag{51}$$

where:

$$T \approx \ell_p/(k_{ex} - \beta_{eff}) \tag{52}$$

Here ℓ_p is the effective lifetime of a prompt neutron in the reactor, and $k_{ex} = k_{eff}\,(+0)-1$. The reactivity in dollars is defined as:

$$\rho = k_{ex}/\beta_{eff} \tag{53}$$

A value of $\rho = \$1$ thus implies prompt criticality.

A reactor containing U-235 + U-238 will go prompt critical for some value of k_{ex} between 0.0065 and 0.0157. If the reactor is thermal (i.e., most fissions are of the U-235), prompt criticality occurs at $k_{ex} \approx 0.0065$. In a fast reactor containing Pu-239 + U-238, where the majority of the fissions are of the Pu-239, prompt criticality occurs at $k_{ex} \approx 0.0035$. Besides going prompt critical with smaller insertions of reactivity, a fast reactor suffers the further serious disadvantage of having $\ell_p \approx 5 \times 10^{-7}$sec,[20] vs. about 10^{-4} - 10^{-5}sec for a large thermal reactor. In a large fast reactor having $\ell_p = 5 \times 10^{-7}$sec, the hypothetical step addition of $k_{ex} = 0.007$, i.e., $\sim$0.0035 above prompt critical, would result in a doubling of the power every 100 microseconds.

Although it is relatively easy to calculate step changes in reactivity for a number of hypothetical cases, it is difficult to attach physical meaning to such reactivity insertions. This difficulty arises because physical processes leading to reactivity insertions take place over significant lengths of time, and also because the process of adding reactivity perturbs the state of the reactor, which in turn perturbs the mechanism of reactivity insertion. Sodium voiding is constrained by inertial effects and possibly choking of two-phase flow, and the Doppler and expansion effects are controlled by heat transfer in the core. Hence, there is strong coupling between a malfunction causing a reactivity change, the rate at which the power

increases, and the subsequent time and spatial perturbation of the reactor composition.

An accident model must thus take into account the neutronic, thermal-hydraulic and mechanical couplings involved. At present this is done only in a rather crude manner, due to the great complexities of the interacting processes. For example, the pertinent neutronics calculations are almost always made using a point (i.e., space-independent) kinetics model. Only rather recently have attempts been made to treat spatial kinetics effects. Similarly, the problems of treating superheat and two-phase choked flow in sodium are only beginning to be understood. Materials properties required for accident calculations may change with irradiation. Thus, the coring of oxide fuel mentioned earlier leads to changes in the radial temperature distribution in the fuel. A number of computer codes based upon simplified calculational models have been developed; these include AX-1,[21] FORE-II,[22] and AIROS II-A.[23]

Fast reactor accidents are usually assumed to be initiated by a power increase at constant flow, or local or corewide flow reduction at constant power. The power increase could be caused, for example, by a fuel subassembly falling into a just subcritical core during refueling. Local flow reduction could be caused by a foreign object that impedes the coolant flow to one or more subassemblies. Corewide flow reduction could result from massive breaks in the primary loop, or primary pump failure.

The conceivable sequences of events following such an initiating mechanism in a fast reactor accident depend strongly on the modes of accident termination specified and points in time when they begin to act. Automatic, fast-acting, redundant control is the most desirable of such modes. As a backup in case of serious control malfunction, it is generally argued that an LMFBR should be designed to have an inherent negative power coefficient of reactivity, i.e., it should become less reactive as its power (and hence, temperature) increases. Even if a reactor is so designed, a rapid-loss-of-coolant accident can lead to core meltdown, due to a high rate of decay heat generation. If core meltdown leads to reassembly to a super-critical configuration, accident termination is due to rapid heating and final core disassembly. This ultimate class of accidents is usually analyzed by means of the Bethe-Tait method, or some modification of it.[24]

Unless reliable failure detection instrumentation is used on each subassembly of a core, initial malfunctioning of an individual subassembly

may be very difficult to detect. It is thus important to study the mode and extent of failure propagation from element to element within a subassembly, and from subassembly to adjacent subassembly. It is conceivable that propagation of local failure, e.g., via fission gas blanketing, can lead to at least local core meltdown, whether or not the reactor has a negative power coefficient of reactivity. A rather detailed picture of safety work on LMFBRs is given in the Proceedings of the Conference on Safety, Fuels, and Core Design in Large Fast Power Reactors held at Argonne National Laboratory on October 11-14, 1965 (ANL-7120).

B. Sodium Void Effect

The removal of sodium from a large U-Pu fueled critical LMFBR has the following neutronic effects:

1. Reduction in the parasitic capture of neutrons by sodium.
2. Increase in the neutron leakage rate caused by the increase in the core transparency.
3. Hardening of the neutron spectrum caused by a decrease in elastic and inelastic scattering by sodium.

The first of the above effects results in a small increase in reactivity. The second effect is always negative, but its magnitude depends upon the location and size of the voided volume -- a void near the center does not have as great a leakage effect as the same size void near the edge of the core. The third effect results in a decrease in neutron captures by all reactor materials, together with a less rapid decrease in Pu-239 fissions and an increase in U-238 fissions. The net effect is always positive.

The net sodium void effect is the sum of the above individual effects, and may be positive or negative, depending upon a number of factors. If the reactor is small and has a relatively hard spectrum to begin with, the leakage dominates, and the void effect is negative. As the reactor size increases, the core acts increasingly as its own reflector; leakage thus becomes less and less important, and the positive hardening effect dominates. The trend for oxide-, carbide-, and metal-fueled reactors is illustrated in Fig. 9

Scales for the ordinate and abscissa of the foregoing sketch are not given because the actual value of the void effect depends upon the specific reactor configuration, its relative fuel, structure, and coolant content, and its fuel type. Similar configurations and volume fractions are assumed in Fig. 9.

In Table III a comparison is made of two-core-zone reactors fueled with oxide, carbide, and metal, at H/Ds of 0.8 and 0.4. (Table IV gives the

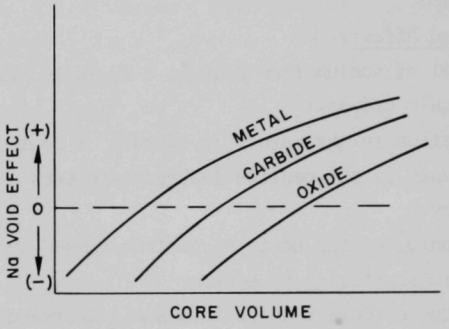

Fig. 9 Trend of sodium void effect with core volume and fuel type

TABLE III

Comparison of Neutronics Parameters for

1000 MWe Two-core-zone Oxide, Carbide, and Metal Fuel LMFBRs

	Oxide	Carbide A	Carbide B	Metal
H/D = 0.8				
v_f, core	0.2966	0.2242	0.3203	0.2560
$(P_{max}/P_{avg})_{radial}$	1.210	1.215	1.206	1.200
M_c, kg(Pu-239 + Pu-241)	1787	1740	2008	1749
CR_i*	0.913	0.917	1.153	0.979
CR_o	0.626	0.627	0.786	0.662
BR	1.225	1.335	1.466	1.360
$(\Delta k/k)_{Na,i}$	+0.02030	+0.01841	+0.02321	+0.02754
$(\Delta k/k)_{Na,o}$	-0.00276	-0.00631	+0.00044	-0.00035
$(\Delta k/k)_{Na,i+o}$	+0.01754	+0.01211	+0.02366	+0.02719
$\bar{E}$**, keV	132	163	171	199
H/D = 0.4				
v_f, core	0.2966	0.2242	0.3203	0.2560
$(P_{max}/P_{avg})_{radial}$	1.232	1.215	1.236	1.219
M_c, kg(Pu-239 + Pu-241)	1863	1840	2092	1854
CR_i	0.847	0.831	1.065	0.880
CR_o	0.626	0.611	0.784	0.642
BR	1.129	1.305	1.460	1.326
$(\Delta k/k)_{Na,i}$	+0.00616	-0.00150	+0.01016	+0.00800
$(\Delta k/k)_{Na,o}$	-0.00801	-0.01513	-0.00378	-0.00813
$(\Delta k/k)_{Na,i+o}$	-0.00185	-0.01663	+0.00638	-0.00014
$A_{Dop,i+o}$***	-0.0081	-0.0059	-0.0059	-0.0029
$\bar{E}$, keV	140	175	181	212

* Subscript i → inner core zone; o → outer core zone
** Median energy in core for flux
*** $A_{Dop} = T\, dk/dT$

TABLE IV. Background Assumptions for Neutronics Comparison of LMFBR Types

Parameter	Oxide	Carbide A	Carbide B	Metal
Fuel	UO_2-PuO_2	UC-PuC	UC-PuC	U-Pu-10 w/o Zr
Fuel density, gms/cm^3	0.80 × 11.1	0.80 × 13.6	0.80 × 13.6	0.70 × 16.0
Midcycle burnup, MWd/ton*	50,000	50,000	50,000	45,000
Fuel full-power life, yrs	1.75	1.75	2.50	1.75
Fuel avg. linear power, kW/ft	10.5	16.0	16.0	8.0
Fuel pin dia., in.	0.225	0.241	0.288	0.182
Fuel element dia., in.	0.255	0.271	0.318	0.212

*100,000 MWd/ton = 11.02%

Further assumptions common to all four reactors were:

1. Reactor thermal power = 2500 MW.
2. Core power/reactor power = 0.9.
3. Average core power density = 400 kW/liter.
4. Pu-239:Pu-240:Pu-241:Pu-242 = 1.0:0.4:0.07:0.
5. Axial blanket thickness = 45.72 cm; volume fractions same as core; heavy atoms = 99.5% U-238, 0.5% Pu-239.
6. Radial blanket thickness = 38.10 cm; $v_f = 0.50$, $v_s = 0.17$, $v_{Na} = 0.33$; heavy atoms = 98% U-238, 2% Pu-239.
7. Reflector thickness = 15.0 cm; $v_s = 0.50$, $v_{Na} = 0.50$.
8. Na void effect for 100% removal of sodium from given core zone and associated axial blanket; perturbation theory.
9. Doppler effect calculated for heating of U-238 from 300 to 750°K; sodium in.
10. Cross-section library: ANL-224.

design assumptions used in making the neutronics calculations.) Table III shows that for the hypothetical case of instantaneous uniform removal of 100% of the sodium from the inner core zone and associated axial blanket, important step increases in k_{eff} generally occur. The most serious increases are for the higher H/D cores, because in these the leakage component is relatively small. This suggests that by designing a core that is inherently leaky upon voiding (i.e., that has a relatively large surface-to-volume ratio), one can reduce the void effect. Such spoiled geometries are achieved with pancake, annular, and modular reactors. These spoiled-geometry reactors have a major drawback, however; critical mass and doubling time increase with the extent of spoiling. More is said of these specifically in Section VII.

The atom densities of the oxygen in the oxide fuel and the carbon in the carbide fuel are similar to that of the sodium. Thus, when sodium voiding occurs in such reactors, a significant amount of low atomic mass scattering material remains. In a metal fuel reactor, however, this is not the case, so the spectral hardening component of the void effect is greater. This results in relatively large sodium void effects for metal fuel reactors, as is shown in Table III.

At this point, it seems reasonable to ask whether there are other reasonable coolants than sodium. Helium has been investigated by Gulf General Atomic Corp., Oak Ridge National Laboratory, and others. Its primary advantage has been suggested to be a reduced degradation of the neutron spectrum, resulting in both improved breeding and reduced coolant void effects. The average core power density in a helium-cooled breeder appears to be ~220 kW/liter, vs. about 500 kW/liter for a sodium-cooled breeder. This implies that for a given thremal power, the volume of a helium-cooled breeder must be about double that of an equivalent sodium-cooled breeder, which in turn results in a larger critical mass for the helium system. Hence, the helium breeder must have a good breeding gain to be competitive with the sodium breeder. Studies by both Gulf General Atomic and Oak Ridge suggest a breeding gain of about 0.5 for 1000 MWe systems; the corresponding doubling time is 8-9 years. The corresponding total void effect for helium is about 0.005 $\Delta k/k$, but the rate of voiding may well be slow, relative to sodium. Thus, helium offers promise as an alternate coolant.[25]

Steam is also under investigation as a potential coolant for fast breeders. Its major advantage is association with a well-developed technology; this must be weighed against an inherently poor breeding gain because of the moderating effect of the hydrogen in the steam, and a significant

increase in reactivity with decreasing steam density. Other gaseous coolants, including CO_2 and SO_2, have also been proposed. The former looks attractive if it proves stable in the reactor radiation field.

Besides considering alternate coolants to alleviate the sodium void problem, one can also consider the use of other fissile-fertile combinations than Pu-239-U-238. The total energy content of the world's thorium resources has been estimated to be about double that of the world's uranium resources. A breeder reactor using U-233 fuel in Th-232 has the advantage of having a sodium void effect whose spectral hardening component is relatively small. This is because $\alpha \equiv \sigma_c/\sigma_f$ for U-233 is rather flat over the range 5 keV-1 MeV (see Fig. 6), and σ_f for Th-232 has a relatively high threshold and small magnitude (see Fig. 5). Such a reactor exhibits negative sodium void effects.[20] It has relatively poor breeding characteristics, however, and also has serious control and fuel reprocessing problems. The poor bredding characteristics are largely due to the relatively low neutron yield per fission, ν, in the U-233, and the consequent high fuel enrichment. The control problems relate to the inherently low conversion ratio, resulting in significant reactivity swings between reloadings and the buildup of U-233 during shutdowns, because of the relatively long half-life of its Pa-233 precursor:

$$\text{Th-232} \xrightarrow{(n,\gamma)} \text{Th-233} \xrightarrow[22\text{m}]{\beta^-} \text{Pa-233} \xrightarrow[27\text{d}]{\beta^-} \text{U-233}$$

(Note in Section III that the Np-239 precursor of Pu-239 has a half-life of only 2.3 days.)

In a large Pu-239-U-238-fueled breeder, the sodium void effect per unit volume is most positive at the center of the core. It decreases with increasing distance from the center, and goes negative at some point. This has led to the suggestion of a dual-fuel-cycle breeder, utilizing an inner U-233-Th-232 core and an outer Pu-239-U-238 core.[26] Here the inner core would be made just large enough to handle the void effect. Such a reactor would have somewhat better breeding characteristics than one using the pure U-233-Th-232 cycle, but would also still have serious control and fuel reprocessing problems.

C. Doppler Effect

Let the cross section of an absorber around a resonance have a shape similar to that sketched in Fig. 10. Here E is the energy corresponding to the velocity of the neutron relative to the target nucleus. If the nucleus is at rest, the velocity is simply that of the neutron in the Laboratory System.

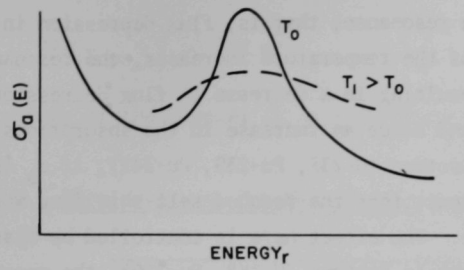

Fig. 10 Absorption cross section around a resonance

If the nucleus is in motion (e.g., periodic vibration of atoms in a crystal lattice), then the relative velocity assumes a range of values; i.e., to the nucleus, the neutron appears to have a range of energies. This means that neutrons that would be outside the range of resonance absorption for stationary nuclei may now fall within the range. This is known as Doppler broadening of the resonance. The faster the nuclei move, i.e., the higher their temperature, the wider the broadening.

It can be shown with the Breit-Wigner formula that the area under the above resonance is independent of Doppler broadening; i.e., the increase in width is accompanied by a corresponding decrease in the cross-section peak. Consider now the absorption cross section as a function of relative neutron energy for heavy nuclide x, and the corresponding distribution of flux at some $\vec{r}_0$, $\phi(E,\vec{r}_0)$, as sketched in Fig. 11. At the lower absorber temperature, T_0,

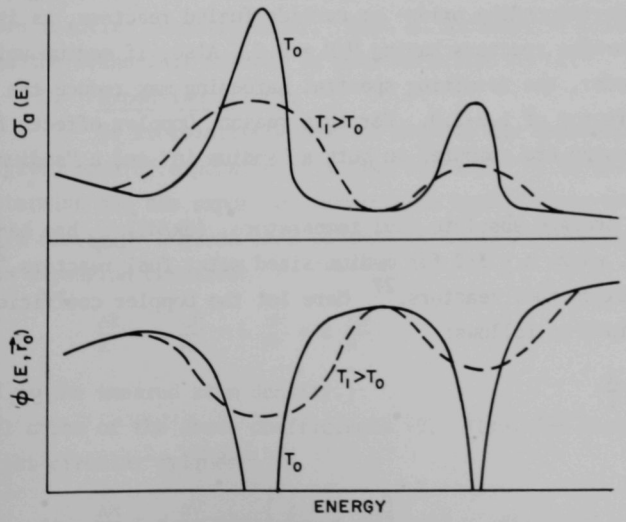

Fig. 11 Absorption cross section and flux in a resonance region

self-shielding occurs at each resonance; that is, flux depression in a resonance reduces absorptions in it. As the temperature increases, the resonances broaden but decrease in magnitude, resulting in a decrease in flux depression or self-shielding in the resonance, and hence an increase in the absorptions. In the case of a thermally fissile isotope (U-235, Pu-239, Pu-241), if σ_a is predominantly the fission component, then the reduced self-shielding would correspond to a reactivity increase. The effect here is controlled by fission vs. capture. In the case of a fertile isotope (U-238, Pu-240), the resonances are far below the fission threshold (see Section I), and σ_a is predominantly capture. This results in a reactivity decrease with increasing temperature.

An increase in the temperature of U-238-Pu fast reactor fuel generally results in a net decrease in reactivity caused by the Doppler effect, mainly because of increased captures in the U-238. It is noteworthy that for the U-238 Doppler to be as prompt-acting as possible, the U-238 must be thermally closely coupled to the primary heat-producing Pu-239. That is, significant segregation of the fuel species caused by fabrication or thermal migration during operation is undesirable.

As stated in the Introduction, it is predominantly the flux in the 1 keV region that contributes to the Doppler effect. Thus, the more moderating material an LMFBR core contains (i.e., the softer its spectrum), the greater should be its Doppler effect. This implies that a metal-fueled reactor that does not contain specially introduced moderating material will have a smaller Doppler effect than corresponding oxide- or carbide-fueled reactors, as is shown in Table III for the reactors having H/D = 0.4. Also, if sodium voiding occurs in a fast breeder, the resulting spectral hardening may reduce the Doppler effect by a factor of 1.5-2.0. For this reason, Doppler effects for a particular reactor design are computed on both a "sodium in" and a "sodium out" basis.

With T the average absolute fuel temperature, $(dk/dT)_{Dop}$ has been taken to vary as T^{-n}, where $n \leq 3/2$ for medium-sized metal fuel reactors,[24] and $n \simeq 1$ for large oxide fuel reactors.[27] Here let the Doppler coefficient A, for $n = 1$, be defined as follows:

$$\left[\frac{dk}{dT}\right]_{Dop} = \frac{A}{T} \qquad (54)$$

or:

$$(\Delta k)_{Dop} = 2.3A \log \frac{T_2}{T_1} \tag{55}$$

The magnitude of the Doppler Δk as a function of A and T_2/T_1 is shown in Table V.

TABLE V. Doppler Δk vs. Doppler Coefficient and Fuel Temperature Ratio

T_1/T_2 \ A	-0.001	-0.004	-0.007
1.5	-.0004	-.0016	-.0028
2.0	-.0007	-.0028	-.0049
2.5	-.0009	-.0037	-.0065

Massive melting of oxide fuel will occur for T_2/T_1 in the range 1.5-2.0, and for carbide and metal fuel at progressively lower values. For A typically $\sim$-0.004, it is seen that the Doppler effect provides a relatively small reactivity feedback at temperatures below which massive fuel melting takes place. The major value of the Doppler effect, then, is to limit the ultimate energy release in an accident in which fuel melting and rearrangement to a more reactive geometry occur. Such an accident is traditionally analyzed via the Bethe-Tait method, or some variation of it.[24]

D. Expansion Effects

It is relatively easy to compute the reactivity effect caused by a given mode of expansion of a fast reactor. It is not easy, however, to determine how the expansion varies with time. Thus, we consider only the $\Delta k/k$ caused by a given $\Delta R/R$ or $\Delta H/H$ or both, without speculating as to how the expansion occurred:

$$\frac{\Delta k}{k} = a \frac{\Delta R}{R} + b \frac{\Delta H}{H} + c \frac{\Delta N}{N} \tag{56}$$

(N is the smeared atom density.)

All three of the above coefficients >0. Also, for thermal expansion of a right circular cylinder:

$$\frac{\Delta N}{N} = -\frac{\Delta V}{V} = -\left[\frac{2\Delta R}{R} + \frac{\Delta H}{H}\right] \tag{57}$$

TABLE VI

Comparison of Characteristics of Fast Breeder Reactors Assuming Low and High α of ^{239}Pu

	Critical Enrichment (% fissile)		Breeding Ratio		Doppler Coefficient $T\frac{dk}{dT}$		Δk 40% Loss of Sodium		Median Energy of Flux (keV)	
	low α	high α	low α	high α	low α	high α	low α	high α	low α	high α
Softer Spectrum Cores[a]										
Oxide[b]	15.8	16.5	1.25	1.10	-0.0056	-0.0041	-0.0024	0.0023	147	153
Carbide[b]	13.1	13.6	1.42	1.27	-0.0053	-0.0040	0.0011	0.0048	175	182
Metal[b]	14.5	14.8	1.35	1.25	-0.0026	-0.0020	0.0006	0.0044	208	212
Gas Cooled[b]	16.7	17.1	1.21	1.12	-0.0023	-0.0017	-	-	210	215
Oxide-High Density[c]	13.2	13.7	1.44	1.29	-0.0052	-0.0039	0.0017	0.0039	156	161
Gas Cooled-High Density[c]	13.2	13.6	1.50	1.37	-0.0034	-0.0025	-	-	182	187
Harder Spectrum Cores[d]										
Oxide[b]	24.0	25.1	1.29	1.15	-0.0031	-0.0022	0.0022	0.0052	175	183
Carbide[b]	19.8	20.5	1.47	1.33	-0.0031	-0.0023	0.0035	0.0060	206	212
Metal[b]	21.9	22.4	1.37	1.28	-0.0016	-0.0012	0.0061	0.0087	231	235
Oxide-High Density[c]	18.0	18.6	1.50	1.36	-0.0034	-0.0025	0.0027	0.0042	177	184

[a]Based on spherical calculations, core volume 1826 liters (1228 liters for high density).
[b]Core and blanket 29.7 vol% fuel, 14.7 vol% stainless steel, 55.7 vol% coolant (smear densities 85% for oxide and carbide, 70% for 12 wt% zirconium-alloyed metal fuel, fission-product pairs 5.7 at.% of heavy atoms).
[c]Core and blanket 44.5 vol% fuel, 20.7 vol% stainless steel, 34.7 vol% coolant.
[d]Based on slab calculations 30-cm core height.

Thus:

$$\frac{\Delta k}{k} = a\,\frac{\Delta R}{R} + b\,\frac{\Delta H}{H} - c\,\left(\frac{2\Delta R}{R} + \frac{\Delta H}{H}\right) \qquad (58)$$

The magnitudes of a, b, and c depend upon R, H, and the reactor composition, but the third term always dominates, making $\Delta k/k < 0$. Radial and axial expansion effects vs. core H/D are shown in Fig. 12. Both sets of curves correspond to $\Delta N/N = -2\%$. It is seen that for a given $-\Delta N/N$, radial expansion produces a more negative $\Delta k/k$, except for H/D $\tilde{>}$0.9. Most LMFBRs are designed with H/D $\tilde{<}$ 0.4. Thus, if expansion is used as a mode of shutdown, radial expansion is preferable if it can be made fast-acting.

E. Effects of Nuclear Uncertainties

Effects of uncertainties in nuclear parameters on breeding and fuel cycle costs were mentioned in Section I. These uncertainties also affect the calculation of the Doppler coefficient and sodium void effect. Table VI shows this for high and low values of α for Pu-239. The sensitivity of the sodium void effect is particularly noteworthy.

Effects of uncertainties in other nuclear parameters, as well as α for Pu-239, are given in Table VII. These calculations are for a reactor designed solely on the basis of thermal-hydraulics and economics considerations, as mentioned at the end of Section I.

TABLE VII.[4] Doppler and Total Na Void Uncertainty Ranges (2.5-ft Core)

Data Uncertainty	Doppler $-T[(dk)/(dT)] \times 10^3$	Sodium Void (% Δk)
Pu-239 alpha (0.2 to 15 keV)	3.1 to 4.0	1.1 to 1.8
Pu-239 σ_f (15 to 300 keV)	3.7 to 3.9	1.2 to 1.4
Pu-239 $\bar{\nu}$ (0 to 10 MeV)	3.8 to 3.8	1.2 to 1.2
U-238 σ_c (1 to 100 keV)	3.2 to 4.4	1.0 to 1.4
U-238 σ_{incl} (0.1 to 2 MeV)	3.7 to 3.9	1.2 to 1.2
Fission product σ_c (0 to 10 MeV)	3.5 to 4.0	1.1 to 1.3
All data uncertainties	2.8 to 4.6	0.9 to 1.9
Base values (ENDF/B)	3.8	1.2

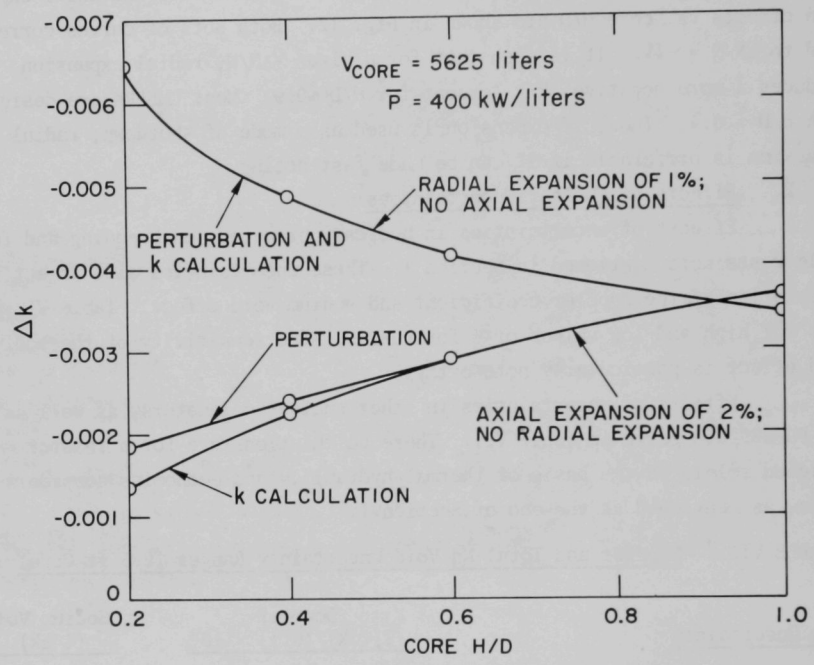

Fig. 12 Expansion effects vs core H/D.

It is seen here that the major contributors to uncertainty in the Doppler coefficient are α for Pu-239 and σ_c for U-238, and that the former is the major contributor to uncertainty in the sodium void calculation.

VII. Design Approaches

A. Background

The first LMFBRs designed to operate at thermal power levels greater than a few megawatts were the Dounreay Fast Reactor (72 Mw), the Experimental Breeder Reactor-II (62.5 Mw), and the Enrico Fermi (200 Mw); their initial core volumes were approximately 130, 73, and 379 liters, respectively. In these relatively small reactors the sodium void effect was dominated by its leakage component, i.e., it was negative. With these reactors the primary safety problem was felt to be core meltdown and reassembly to a more reactive configuration.[28] This concern had been emphasized by the meltdown of the EBR-I core in November, 1955 (in that case a severe excursion did not occur).[29] The classical Bethe-Tait method and modifications of it were developed to handle this class of problem.[24] Studies based on this method predict that the total energy release in a meltdown accident corresponding to a constant reactivity insertion rate does not depend strongly upon the initial reactor power level or the magnitude of the prompt neutron lifetime. The energy release is strongly affected, however, by the Doppler feedback.

As LMFBR design studies become oriented toward larger size reactors, notably those required for 1000 MWe power plants, it was found that such reactors might have large positive sodium void effects.[30] As a result, a great deal of work was done to reduce or eliminate this problem. Two general approaches were proposed: material and geometric core spoiling. The aim of material spoiling is primarily to enhance the sodium-out Doppler coefficient by introducing a permanent moderator such as beryllium into the core.

In geometric spoiling, the core surface-to-volume ratio is increased to enhance the leakage component of the sodium effect. Three types of reactor design based upon geometric spoiling have been proposed -- pancake, annular, and modular. A pancake reactor is one whose core $H/D \lesssim 0.35$. A relatively large fraction of its neutron leakage is into its axial blankets, which therefore contribute appreciably to its breeding ability and power generation. Because of its relatively short height, a low ΔP is readily achieved across a pancake core. Alternatively, one may choose to decrease the coolant volume fraction, thereby increasing the ΔP, and thus increase the fuel volume fraction to improve breeding in this reactor.

An annular reactor is one whose core is an annulus, generally surrounded on both sides by radial blankets. These blankets contribute appreciably to the breeding and power generation in this reactor, and thus complicate the distribution of coolant flow with time. An economic advantage of the annular reactor is that it has taller and fewer fuel elements, which reduces fuel fabrication costs.

A modular reactor consists in principle of two or more core modules, each partially surrounded by its own radial blanket, that are coupled neutronically. In practice, designs have been developed for three- to seven-module reactors. With these, as with the annular designs, a significant fraction of breeding and power generation takes place in the radial blankets, and there are the same coolant distribution problems. Modular reactors are difficult to analyze neutronically, because of θ-variation (in r-θ-z coordinates) of their radial boundary conditions; here even two-dimensional diffusion theory is not truly descriptive. Thus, reactivity effects, such as sodium voiding in regions directly between two modules, are difficult to evaluate. The particular effect cited could give rise to a serious increase in neutronic coupling between modules. The θ-variation of radial blanket power in a modular reactor also seriously complicates the distribution of coolant flow in the radial blankets.

All of the spoiling techniques cited, material or geometric or both, lead to such economic penalties that it is now accepted that significant spoiling is intolerable in the long run. But designing to a near-zero or negative sodium void effect is not only bad economically; it is now generally taken to represent a simplistic approach to fast reactor safety. Two important points in this latter regard were made in the previous section:

1. It is the realistic rate of sodium voiding that must be considered in an LMFBR accident; a reactivity change due to an overall step removal of the coolant has little physical significance.

2. Even if an LMFBR is designed to have a near-zero or negative sodium void effect, it can still melt down.

Thus, current studies in fast reactor safety are aimed at getting a better understanding of the interacting kinetic effects (neutronic, thermal-hydraulic and mechanical) taking place during a reactor malfunction, as a rational basis for design. A detailed description of the LMFBR Safety Program is given in Volume 10 of the LMFBR Program Plan.[31]

B. Core Design

Designing an LMFBR plant to meet specified overall plant economic and safety requirements involves work in the following areas:

1. materials
2. neutronics
3. thermal-hydraulics
4. structural mechanics
5. safety
6. cost analysis

Since the work in these areas is strongly interrelated, the final design is arrived at by an increasingly detailed iterative process.

A major goal of related materials work is the ability to predict the burnup capability of a proposed fuel element. This involves not only the determination of materials properties, but the use of these properties in complex structural mechanical models of fuel element behavior under reactor operating conditions. These fuel lifetime models are translated into computer codes (e.g., BULGE, CYGRO, NUKER and SWELL) for use in design trade-off studies.[32] Here, for example, the smeared density of the fuel in the element is a key parameter. If the density approaches the theoretical limit, maximum breeding results - at the start of operation. But the lack of void space to accommodate fission products leads to a short lifetime for the element. A proper balance is ultimately determined by an overall cost analysis. This is because other factors must be considered, such as the fuel management scheme, heat transfer and safety. The thermal performance of representative fuel element designs is shown in Table VIII.

An important aspect of the neutronics calculations is the determination of the shift with time of the power distribution in the reactor, as discussed in Section V. This shift is related not only to fuel management and thermal-hydraulics considerations (e.g., how do peak fuel temperatures shift with time), but also to the optimum location of control elements. Another important aspect is safety-oriented kinetics calculations; these provide background for instrumentation specification and design of control rod drives.

Thermal-hydraulics calculations are used to study different methods for spacing fuel elements, as well as to determine fuel element pitch. The spacing methods include helically wrapped wires and various forms of intermittent grids. Here, axial support interval as it relates

Table VIII, Thermal Performance of Representative Fuel Elements

Fuel Composition	Fuel-Element Design Description	Heavy Atom Density, Cold Smeared (%TD)	Heavy Atom Density, Normalized	Fuel Temp. Design Limit, (C)	$\int_{T_C}^{T_{DL}} k dT$[a] (watts/cm)	Linear Power Rating Design Limit in 0.25 in. OD Element with 0.015 in. Wall (kw/ft)[b]	Typical Over-Power Factor	Typical Max. Full Power Rating, (kw/ft)
Most Highly Developed Design—Near Term Missions								
$(Pu_{0.2}U_{0.8})O_{1.98}$	Helium bonded,	80	0.94					
	solid pellet, small	85*	1.00	2700[c]	58	21[d]	1.10-1.25	17-19
	cold diametral gap	90	1.06					
Candidates for Improved Performance—Long Term Missions								
$(Pu_{0.2}U_{0.8})C$	Helium bonded,	70	1.10					
Hyperstoichiometric	solid pellet, small	80*	1.26	2480[c]	281[e]	52	1.25-1.50	35-42
	cold diametral gap	90	1.42					
$(Pu_{0.2}U_{0.8})C$	Sodium bonded,	70	1.10					
Initially hypostoichiometric	solid pellet, large	75*	1.18	1285[f]	82[g]	30	1.05-1.15	26-28
fuel with stabilizing additives	sodium annulus	80	1.26					
Metallic alloy	Sodium bonded, cast	70	1.23					
Ref. comp. 15 w/o Pu	rod, large sodium	75*	1.31	1155[c]	83[g]	30	1.25-150	20-24
10 w/o Zr	annulus	80	1.40					
Bal. U								

*Most probable smeared density.

[a] Thermal conductivity times differential temperature integrated over the temperature range from peak inside cladding temperature (with HCF) at core midplane (assumed to be 600°C) to the fuel temperature design limit (end of life).

[b] Temperature drop from fuel OD to cladding ID calculated on basis of h = 1 watt/(cm^2)(C) for He bond, h = 17 watts/(cm^2)(C) for Na bond (in 0.25 in. OD element with 0.015 in. wall).

[c] Solidus temperature.

[d] Assuming central hole permits 25% higher heat generation than solid rod for the same ΔT.

[e] Assuming 25% degradation of virgin thermal conductivity due to maximum decrease in fuel density within unstrained cladding.

[f] Lowest possible eutectic temperature of intermetallic compounds involving additives and fissile or fertile elements.

[g] Assuming 40% degradation of virgin thermal conductivity due to maximum decrease in fuel density within unstrained cladding.

to subassembly deflection due to radial thermal-gradient-induced bowing must be considered; this involves strong interaction with structural mechanics analysis. Thermal-hydraulics calculations are also used to determine subassembly coolant orificing requirements corresponding to a given, flattened radial power distribution (see Section IV). Orifices are sized to achieve either a constant bulk outlet coolant temperature from all subassemblies, or a uniform maximum clad temperature in all subassemblies; here the shift of power distribution with time must be considered. An important aspect of thermal-hydraulics calculations is the specification of hot-channel and hot-spot factors.[33] These factors are closely related to economic and safety considerations, i.e., whether they are combined statistically or multiplicatively.

The final core design is based upon many structural mechanical analyses, beginning with the fuel element, as mentioned earlier, and including the subassembly, support plate, reactor primary vessel, etc. To enhance breeding, it is desirable to minimize the volume fraction of structural material (fuel element cladding, spacers, subassembly can, etc.) in the core. Excessive structural material takes up space that could be occupied by fuel, and also contributes to parasitic neutron capture. Inadequate structure, on the other hand, could lead to dynamic instability of the reactor. Structural mechanical analyses are necessary in the design of lateral and vertical support for the core. Such support is required to maintain a reproducible reactor geometry from startup to full-power operating conditions, because of expansion effects on reactivity (see Section VI).

C. Control

Steady-state operation in a reactor represents a balance between neutron production and loss by leakage and absorption; reactor control is effected by changing one of these terms. In a small reactor, leakage control can be by means of blanket or reflector movement. With intermediate-size LMFBRs, e.g., the Dounreay Fast Reactor and Experimental Breeder Reactor-II, reflector movement becomes impractical. Here neutron production is controlled by means of fuel-containing control elements. In still larger LMFBRs, control is by means of neutron absorption, i.e., the use of poison in control elements.[34]

Table IX shows the relative worth per unit volume of various control materials (at 90% of theoretical density) in soft and hard neutron spectra.

TABLE IX. A Comparison of Fast Reactor Control Materials[35]

Control Material (2 Inch Rod)	State	Δk/k Soft Spectrum Percent (a)	Δk/k Hard Spectrum Percent (b)
Boron (Natural)	B_4C	7.3	6.7
Europium	Eu_2O_3	5.5	4.6
Gadolinium	Gd_2O_3	3.0	---
Samarium	Sm_2O_3	2.8	---
Hafnium	H_f (Metal)	2.8	---
Tantalum	Ta (Metal)	4.4	3.7
Rhenium	Re (Metal)	6.0	5.1
Tungsten	W (Metal)	2.2	---

(a) Mean Fission Energy - 138 keV.
Cell Composition: 35 v/o Sodium, 35 v/o Fuel, 20 v/o Steel and 10 v/o BeO.

(b) Mean Fission Energy - 246 keV.
Cell Composition: 45 v/o Sodium, 35 v/o Fuel, and 20 v/o Steel.

On the basis of relative worth, properties and cost, boron carbide and tantalum are the most favored of the materials in the above table. Of the two, the boron carbide has the greater worth. It reacts, however, with neutrons to produce helium:

$$_5B^{10} + {}_0n^1 \rightarrow {}_3Li^7 + {}_2He^4$$

Significant helium production causes unacceptable swelling of a control element. Thus, current practice is to specify tantalum for burnup control elements that normally remain in the core, and boron carbide for safety elements that are normally in a withdrawn position.

In Section IV mention was made of using the burnup control elements to help offset the shift of radial power distribution with time in a zoned core. This is done by placing the burnup control elements in the region of peak power density in the outer zone of a two-zone core.

The minimum excess reactivity that must be present in the reactor initially is the sum of that required to go from cold, zero-power critical

to hot, full-power critical, plus that required to compensate for fuel burnup over an operating cycle. The former may be about 2-4% $\Delta k/k$, and the latter, with appropriate design, may be about 0.5-2% $\Delta k/k$. In addition, a reserve of about 2-4% $\Delta k/k$ is specified.

D. Current LMFBR Designs

Five industrial organizations in the U.S. are currently doing design studies of 1000 MWe LMFBR power plants. The major aim of these studies has been to identify the technological problems associated with building an LMFBR plant, but they have also involved work in system optimization. It is work in this latter area that has led to the rejection of core spoiling mentioned at the beginning of this section. Something of a design consensus is beginning to emerge, although there are still significant points of difference. For example, three of the five organizations are basing their designs on mixed oxide fuel, one is using mixed carbide, and one has been using carbide, but has some interest in oxide. The designs being studied by the five organizations as of early 1968 are shown in Table X, taken from data of reference 32. It should be emphasized that all of these designs are preliminary and subject to modification (this serves to underscore the current fluid state of the LMFBR art). A detailed discussion of current problems and plans relative to LMFBR core design is given in reference 32.

TABLE X. Preliminary 1000 MWe LMFBR Designs, 1968

Description	Atomics International	Babcock and Wilcox	Combustion Engineering	General Electric	Westinghouse Electric
Reactor Power, MWe / MWt	1000 / 2500	1000 / 2420	1000 / 2500	977 / 2345	1074 / 2600
Core Geometry, H/D	Cylindrical 0.536	-- 0.3	Pancake 0.231	Cylindrical 0.44	Modular ~1.26
Core Height, ft.	4.16	2.9	2.0	3.0	3.88
Fuel	$(U,Pu)O_2$	$(U,Pu)O_2$	(U,Pu)C	$(U,Pu)O_2$	(U,Pu)C
Reactor Fissile Inventory, kg Pu_f	2264	2770	2644	2026	---
Reactor Breeding Ratio	~1.30	1.38	1.55	1.37	---
Doubling Time,* yrs.	10.0	10.8	5.9	7.8	6.0
Maximum Linear Power, kw/ft	15	17	43.5	18.1	30.6
Average Core Specific Power, kw/kg fiss.	1260	885	---	1400	---
Average Core Power Density, Kw/liter	400	334-361	---	---	---
Coolant Temperature, °F, inlet / outlet	760 / 1060	800 / 1100	785 / 1090	855 / 1150	750 / 1028
Core ΔP, psi	100	46	150	60	82.7
Maximum Coolant Velocity, fps	32.8	---	40	38.2	28.7

*Simple

References

1. *Reactor Physics Constants*, ANL-5800, 2nd Ed., July 1963.

2. Stehn, J. R. et al, *Neutron Cross Sections, Vol. III, Z-88 to 98*, BNL-325, 2nd Ed., Suppl. No. 2, Feb. 1965.

3. Langner, I., Schmidt, J. J., and Woll, D., *Tables of Evaluated Neutron Cross Sections for Fast Reactor Materials*, KFK-750, January 1968.

4. Greebler, P., Hutchins, B. A., and Linford, R. B., *Sensitivity of Fast-Reactor Economics to Uncertainties in Nuclear Data*, Nuclear Applications, 4, 297, May 1968.

5. Butler, D. K., Bogner, M., and Loewenstein, W. B., *Effects of High Capture-to-Fission Ratio of Pu-239 on the Performance of Fast Breeder Reactors*, Trans. Am. Nucl. Soc., 1968 Annual Meeting, June 10-13, 1968, p. 204.

6. Okrent, D., *Neutron Physics Considerations in Large Fast Reactors*, Power Reactor Technology, 7, 2, 107, Spring 1964.

7. Meneghetti, D., *Introductory Fast Reactor Physics Analysis*, ANL-6809, December 1963.

8. Clark, M., Jr., and Hansen, K. F., *Numerical Methods of Reactor Analysis*, Academic Press, 1964.

9. Greenspan, H., Kelber, C., and Okrent, D., Editors, *Computing Methods in Reactor Physics*, Gordon and Breach Science Publishers, 1968.

10. Glasstone, S., and Edlund, M. C., *The Elements of Nuclear Reactor Theory*, D. Von Nostrand Company, Inc., 1952.

11. Weinberg, A. M., and Wigner, E. P., *The Physical Theory of Neutron Chain Reactors*, The University of Chicago Press, 1958.

12. Okrent, D., *Summary of Intercomparison Calculations Performed in Conjunction with Conference on Safety, Fuels and Core Design in Large Fast Power Reactors*, Proceedings of the Conference on Safety, Fuels and Core Design in Large Fast Power Reactors, October 11-14, 1965, ANL-7120, p. 3.

13. *Reactor Handbook*, 2nd Edition, Vol. III, Part A, Physics, H. Soodak, Ed., Interscience Publishers, 1962.

14. Meneley, D. A., Kvitek, L. C., and O'Shea, D. M., *MACH-I, A One-Dimensional Diffusion-Theory Package*, ANL-7223, June 1966.

15. Long, J. K. et al., *Fast Power Reactor Studies - ZPR-III*, P/598, 12, Reactor Physics, Proceedings of the Second United Nations International Conference on the Peaceful Uses of Atomic Energy, 1 Sept.-13 Sept., 1958, p. 130.

References (Contd.)

16. Perks, M. A., and Lord, R. M., *Effects of Axial and Radial Blanket Design on Breeding and Economics*, Proceedings of the Conference on Breeding, Economics and Safety in Large Fast Power Reactors, October 7-10, 1963, Argonne National Laboratory, ANL-6792, Dec. 1963, p. 367.

17. *Current Status and Future Technical and Economic Potential of Light Water Reactors*, WASH-1082, March, 1968.

18. Link, L. E. et al., *1000-MW(e) Metal-Fueled Fast Breeder Reactor*, ANL-7001, June 1966.

19. *Liquid Metal Fast Breeder Reactor Program Plan*, Vol. 7, Fuels and Materials, WASH-1107, August 1968.

20. Okrent, D., Cohen, K. P., and Loewenstein, W. B., *Some Nuclear and Safety Considerations in the Design of Large Fast Power Reactors*, P/267, Vol. 6, Proceedings of the Third International Conference on the Peaceful Uses of Atomic Energy, Geneva, 1964.

21. Okrent, D. et al., *AX-1, A Computing Program for Coupled Neutronics-Hydrodynamics Calculations on the IBM-704*, ANL-5977, May 1959.

22. Fox, J. N. et al., *FORE-II: A Computational Program for the Analysis of Steady-State and Transient Reactor Performance*, GEAP-5273, September 1966.

23. Blaine, R. A., and Berland, R. F., *Simulation of Reactor Dynamics. Volume I. A Description of AIROS II-A*, NAA-SR-12452, Sept. 5, 1967.

24. Nicholson, R. B., *Methods for Determining the Energy Release in Hypothetical Fast-Reactor Meltdown Accidents*, Nuclear Science and Engineering, 18, 207-219 (1964).

25. Fortescue, P. et al, *Safety Considerations of Large Gas-Cooled Fast Power Reactors*, Proceedings of the Conference on Safety, Fuels, and Core Design in Large Fast Power Reactors, October 11-14, 1965, ANL-7120, p. 230.

26. Loewenstein, W. B., and Blumenthal, B., *Mixed Fuel-Cycle Fast Breeder Reactors; Nuclear, Safety and Materials Considerations*, Proceedings of the Conference on Safety, Fuels and Core Design in Large Fast Power Reactors, October 11-14, 1965, ANL-7120, p. 751.

27. Sherer, D. G., and Meinhardt, W. G., *An Analysis of Fast Reactor Transient Response and Safety in Selected Accidents*, GEAP-4787, June 1966.

28. McCarthy, W. J. et al., *Nuclear Accidents in Fast Power Reactors*, P/2165, 12, Reactor Physics, Proceedings of the Second United Nations International Conference on the Peaceful Uses of Atomic Energy, 1 Sept.-13 Sept., 1958, p. 207.

References (Contd.)

29. Brittan, R. O., *Analysis of the EBR-I Core Meltdown*, P/2156, 12, Reactor Physics, Proceedings of the Second United Nations International Conference on the Peaceful Uses of Atomic Energy, 1 Sept-13 Sept., 1958, p. 267.

30. Hummel, H. H., Phillips, K., and Rago, A., *Calculations of Sodium Void Reactivity Effect for Large Fast Oxide Reactors in Spherical and Slab Geometry*, Proceedings of the Conference on Breeding, Economics and Safety in Large Fast Power Reactors, October 7-10, 1963, ANL-6792, p. 65.

31. *Liquid Metal Fast Breeder Reactor Program Plan, Vol. 10, Safety*, WASH-1110, August 1968.

32. *Liquid Metal Fast Breeder Reactor Program Plan, Vol. 6, Core Design*, WASH-1106, August 1968.

33. Abernathy, F. H., *The Statistical Aspects of Nuclear Reactor Fuel Element Temperature*, Nuclear Science and Engineering, 11, 1961, p. 290.

34. Loewenstein, W. B., *The Control of Fast Reactors: Current Methods and Future Prospects*, Physics and Materials Problems of Reactor Control Rods, International Atomic Energy Agency, Vienna, 1964, p. 633.

35. *Sodium Cooled Reactors Fast Ceramic Reactor Development Program*, Eighteenth Quarterly Report, February-April, 1966, GEAP-5158, August 1966.

Acknowledgments

I am grateful to D. Butler, H. Hummel, and W. Loewenstein for discussions that helped to shape this report, and to M. Stephenson and P. Pizzica for material used in it.

I am especially grateful to D. Meneley and K. Hub for many excellent technical suggestions for improvement of the original draft. These have been incorporated into the report, and contribute strongly to whatever precision of statement it has.

B